

Coherence and correlation properties of a one-dimensional attractive Fermi gas

Iacopo Carusotto^{1,2} and Yvan Castin^{1,*}

¹*Laboratoire Kastler Brossel, École Normale Supérieure,
24 rue Lhomond, 75231 Paris Cedex 05, France*

²*CRS BEC-INFM and Dipartimento di Fisica, Università di Trento, I-38050 Povo, Italy*

(Dated: April 5, 2004)

A recently developed Quantum Monte Carlo algorithm based on the stochastic evolution of Hartree-Fock states has been applied to compute the static correlation functions of a one-dimensional model of attractively interacting two component fermions. The numerical results have been extensively compared to existing approximate approaches. The crossover to a condensate of pairs can be identified as the first-order pair coherence extending throughout the whole size of the system. The possibility of revealing the onset of the transition with other observables such as the density-density correlations or the second-order momentum space correlations is discussed.

PACS numbers: 05.30.Fk, 02.70.Ss

I. INTRODUCTION

The recent developments in the cooling and trapping techniques of neutral atoms have opened the way to the realization of fermionic atomic samples at temperatures well below the degeneracy temperature [1]. This suggests that atomic gases are ideal candidates for the study of the physics of degenerate many-fermion systems. With respect to solid state ones, atomic systems offer in fact a better isolation from external disturbances such as material defects, a better knowledge of the microscopic details of the systems, as well as a wider range of tunability of the parameters, in particular the interparticle interactions. By tuning the external magnetic field around a Feshbach resonance, the atom-atom scattering length a can be varied from $k_F a = -\infty$ to $+\infty$ (k_F being the Fermi momentum) opening the way towards a comprehensive study of the pairing transition both in the regime $a > 0$ in which a Bose-condensate (BEC) of tightly-bound molecules is present, and in the regime $a < 0$ (BCS) in which a condensate of Cooper pairs is formed. Diatomic molecules have been created and observed by several experimental groups [2]. Bose-Einstein condensation of tightly bound diatomic molecules has been recently reported [3]. The crossover region between BEC and BCS is currently under experimental investigation [4] and first evidences of pairing in the crossover region have been reported in [5].

From the theoretical point of view, a large effort is currently made to establish the main features of the pairing for high values of the scattering length $k_F |a| \gg 1$, regime in which the atomic gas shows strong correlations [6, 7, 8]. In particular, the dependence of the transition temperature on the interaction strength in this crossover region is still an open problem.

The present paper reports a numerical study of the condensation of pairs in a regime of relatively strong interactions, so to characterize the consequences of the transition on the different observables of the system and identify specific features which may represent unambiguous signatures of the onset of condensation of pairs.

The calculations have been performed by applying the quantum Monte Carlo (QMC) method developed in [9] to a one-dimensional lattice model of fermions with attractive on-site interactions. A short description of the model under examination is given in sec. II, while the numerical algorithm used for the calculations is presented in sec. III. Numerical results are presented in sec. IV and then extensively compared to the predictions of a perturbative expansion in the interaction coupling constant (sec. V), and of existing approximate approaches (sec. VI), such as the BCS theory [10, 11], two versions of the random phase approximation (RPA) [12, 13] as well as the Nozières Schmitt-Rink theory [6].

Several among the most relevant correlation functions of the Fermi gas have been considered here, in partic-

*Electronic address: Yvan.Castin@lkb.ens.fr

ular the opposite-spin density-density correlation function $\langle \rho_{\downarrow}(x) \rho_{\uparrow}(0) \rangle$, the first-order pair coherence function $\langle \hat{\Psi}_{\downarrow}^{\dagger}(x) \hat{\Psi}_{\uparrow}^{\dagger}(x) \hat{\Psi}_{\uparrow}(0) \hat{\Psi}_{\downarrow}(0) \rangle$ and the second-order momentum space correlation function $\langle \hat{n}_{k\uparrow} \hat{n}_{-k\downarrow} \rangle$. The density-density correlation function has been already the object of several papers studying the experimental signatures of the BCS transition in atomic Fermi systems, e.g. [14], while the first-order pair coherence function is the counterpart, in a non-symmetry-breaking approach, of the order parameter of the phase transition in a Landau-Ginzburg theory [10].

II. THE PHYSICAL SYSTEM

A one-dimensional low energy two-component Fermi gas can be modeled by the Hamiltonian:

$$\mathcal{H} = \sum_{k,\sigma} \frac{\hbar^2 k^2}{2m} \hat{a}_{k\sigma}^{\dagger} \hat{a}_{k\sigma} + g_0 \sum_x dx \hat{\Psi}_{\uparrow}^{\dagger}(x) \hat{\Psi}_{\downarrow}^{\dagger}(x) \hat{\Psi}_{\downarrow}(x) \hat{\Psi}_{\uparrow}(x). \quad (1)$$

The spatial coordinate x runs on a discrete lattice of \mathcal{N} points with periodic boundary conditions; L is the total length of the quantization box and $dx = L/\mathcal{N}$ is the length of the unit cell of the lattice. The spin index runs over the two $\sigma = \uparrow, \downarrow$ spin states. The system is taken as spatially homogeneous, m is the atomic mass, and interactions are modeled by a two-body discrete delta potential with a coupling constant g_0 . The field operators $\hat{\Psi}_{\sigma}(x)$ satisfy the usual fermionic anticommutation relations $\{\hat{\Psi}_{\sigma}(x), \hat{\Psi}_{\sigma'}^{\dagger}(x')\} = \delta_{\sigma,\sigma'} \delta_{x,x'}/dx$ and can be expanded on plane waves according to $\hat{\Psi}_{\sigma}(x) = \sum_k \hat{a}_{k\sigma} e^{ikx}/\sqrt{L}$ with k restricted to the first Brillouin zone of the reciprocal lattice. In order for the discrete model to correctly reproduce the underlying continuous field theory, the grid spacing dx must be smaller than all the relevant length scales of the system, e.g. the thermal wavelength and the mean interparticle spacing. In the present one-dimensional case, the relation between the coupling constant on the lattice and the physical 1D coupling constant g_{1D} is:

$$g_0 = g_{1D} \left(1 + \frac{m g_{1D} dx}{\pi^2 \hbar^2} \right)^{-1}, \quad (2)$$

which, in the limit $dx \ll \pi^2 \hbar^2 / m g_{1D}$ reduces to the expected one $g_0 = g_{1D}$ [15, 16]. This condition is satisfied in the Monte Carlo simulations presented in this paper. We also note that two particles interacting in free space with a attractive delta potential in 1D have a bound state of energy $-m g_{1D}^2 / 4\hbar^2$. In the numerical examples of this paper, the Fermi energy is much larger than this binding energy so that we are not investigating the condensation of preformed pairs but rather a BCS regime.

III. THE QUANTUM MONTE CARLO SCHEME

We assume the gas to be at thermal equilibrium at a temperature T in the canonical ensemble, so that the unnormalized density operator $\rho_{\text{eq}}(\beta) = e^{-\beta \mathcal{H}}$ with $\beta = 1/k_B T$. From textbook statistical physics, we know that such a density operator can be obtained by means of an imaginary-time evolution:

$$\frac{d\rho_{\text{eq}}(\tau)}{d\tau} = -\frac{1}{2} [\mathcal{H} \rho_{\text{eq}}(\tau) + \rho_{\text{eq}}(\tau) \mathcal{H}] \quad (3)$$

during a “time” interval $\tau = 0 \rightarrow \beta$ starting from the initial state corresponding to the infinite temperature case where $\rho_{\text{eq}}(\tau = 0) = \mathbf{1}_N$, $\mathbf{1}$ being the identity matrix in the N -body Hilbert space.

As it has been recently shown in [9], the exact solution of the imaginary-time evolution (3) can be written as a statistical average of Hartree-Fock dyadics of the form:

$$\sigma = |\phi_1^{(1)} \dots \phi_N^{(1)}\rangle \langle \phi_1^{(2)} \dots \phi_N^{(2)}|. \quad (4)$$

For $\alpha = 1, 2$, $\phi_j^{(\alpha)}$ ($j = 1 \dots N$) are Hartree-Fock orbitals for the N fermions, in the sense that:

$$|\phi_1^{(\alpha)} \dots \phi_N^{(\alpha)}\rangle = \hat{a}_{\phi_1^{(\alpha)}}^{\dagger} \dots \hat{a}_{\phi_N^{(\alpha)}}^{\dagger} |0\rangle, \quad (5)$$

the creation operator corresponding to the wavefunction $\phi(x, \sigma)$ being defined as:

$$\hat{a}_\phi^\dagger = \sum_{x, \sigma} dx \phi(x, \sigma) \hat{\Psi}_\sigma^\dagger(x). \quad (6)$$

For the model Hamiltonian (1), the imaginary-time evolution of each of the orbitals $\phi_j^{(\alpha)}$ can be reformulated in terms of Ito stochastic differential equations of the form:

$$\begin{aligned} d\phi_i^{(\alpha)}(x, \sigma) = & -\frac{d\tau}{2} \left\{ \frac{P^2}{2m} \phi_i^{(\alpha)}(x, \sigma) + \right. \\ & + g_0 \sum_j \frac{1}{\|\phi_j^{(\alpha)}\|_2} \left[|\phi_j^{(\alpha)}(x, -\sigma)|^2 \phi_i^{(\alpha)}(x, \sigma) - \phi_j^{(\alpha)*}(x, -\sigma) \phi_j^{(\alpha)}(x, \sigma) \phi_i^{(\alpha)}(x, -\sigma) \right] + \\ & - \frac{g_0}{2} \sum_j \sum_{x', \sigma'} dx' \frac{1}{\|\phi_j^{(\alpha)}\|_2 \|\phi_i^{(\alpha)}\|_2} \left[\phi_i^{(\alpha)*}(x', \sigma') \phi_j^{(\alpha)*}(x', -\sigma') \phi_j^{(\alpha)}(x', -\sigma') \phi_i^{(\alpha)}(x', \sigma') + \right. \\ & \left. - \phi_i^{(\alpha)*}(x', \sigma') \phi_j^{(\alpha)*}(x', -\sigma') \phi_j^{(\alpha)}(x', \sigma') \phi_i^{(\alpha)}(x', -\sigma') \right] \phi_i^{(\alpha)}(x, \sigma) \left. \right\} + dB_i^{(\alpha)}(x, \sigma), \quad (7) \end{aligned}$$

where P represents the momentum operator on the grid and the norm $\|\phi\|$ is defined as $\|\phi\|^2 = \sum_{x\sigma} dx |\phi(x, \sigma)|^2$. The deterministic part is simply the mean-field Hartree-Fock equation in imaginary time, while the correlation functions of the zero-mean noise $dB_i^{(\alpha)}$ are given by:

$$\overline{dB_i^{(\alpha)}(x, \sigma) dB_j^{(\alpha')}(x', \sigma')} = -\frac{g_0}{2 dx} d\tau \mathcal{Q}_\perp^{(\alpha)}(x, \sigma) \mathcal{Q}_\perp^{(\alpha')}(x', \sigma') \left[\phi_i^{(\alpha)}(x, \sigma) \phi_j^{(\alpha')}(x', \sigma') \delta_{\alpha, \alpha'} \delta_{\sigma, -\sigma'} \delta_{x, x'} \right]. \quad (8)$$

The projector $\mathcal{Q}_\perp^{(\alpha)}(x, \sigma)$ projects orthogonally to the subspace spanned by the wavefunctions $\phi_j^{(\alpha)}(x, \sigma)$. A possible noise with the required correlation function (8) is:

$$\begin{pmatrix} dB_i^{(\alpha)}(x, \uparrow) \\ dB_i^{(\alpha)}(x, \downarrow) \end{pmatrix} = \sqrt{-\frac{g_0}{2 dx} d\tau} \mathcal{Q}_\perp^{(\alpha)} \begin{pmatrix} \xi^{(\alpha)}(x) & 0 \\ 0 & \xi^{(\alpha)*}(x) \end{pmatrix} \begin{pmatrix} \phi_i^{(\alpha)}(x, \uparrow) \\ \phi_i^{(\alpha)}(x, \downarrow) \end{pmatrix}, \quad (9)$$

with $\xi^{(\alpha)}(x)$ independent zero-mean Gaussian noises with $\overline{\xi^{(\alpha)}(x) \xi^{(\alpha')}(x')} = 0$, $\overline{\xi^{(\alpha)*}(x) \xi^{(\alpha')}(x')} = \delta_{x, x'} \delta_{\alpha, \alpha'}$. It can be proven [9] that this set of stochastic differential equations reproduces, in the average over the noise, the exact evolution of the Hartree-Fock dyadic σ during $d\tau$:

$$\overline{d\sigma} = -\frac{d\tau}{2} [\mathcal{H}\sigma + \sigma\mathcal{H}]. \quad (10)$$

The initial state $\mathbf{1}_N$ can be written as a functional integral over all possible sets of orthonormal wavefunctions $\{\phi_j^{(0)}(x, \sigma)\}$ ($j = 1 \dots N$):

$$\mathbf{1}_N = \int_1 \mathcal{D}\phi_1^{(0)} \dots \mathcal{D}\phi_N^{(0)} |\phi_1^{(0)} \dots \phi_N^{(0)}\rangle \langle \phi_1^{(0)} \dots \phi_N^{(0)}|. \quad (11)$$

This writing of the identity operator can be used as a starting point for an exact simulation of the fermionic many-body problem. To this purpose, we have to numerically solve the stochastic differential equations (7) for imaginary times going from $\tau = 0$ to $\tau = \beta$. This is done by splitting the imaginary-time interval into a large enough number \mathcal{M} of time steps; $\xi_j^{(\alpha)}(x)$ is the noise terms at the time-step j ($j = 1 \dots \mathcal{M}$) on the site x . The expectation values of any observable at temperature T is then obtained as an average over all the possible values of the initial wavefunctions $\phi_i^{(0)}$ and the elementary noise terms $\xi_j^{(\alpha)}(x)$.

For example, the partition function $\text{Tr}[\rho]$ is obtained as:

$$\text{Tr}[\rho] = \overline{\langle \phi_1^{(2)} \dots \phi_N^{(2)} | \phi_1^{(1)} \dots \phi_N^{(1)} \rangle} \quad (12)$$

or, equivalently, as the determinant $\text{Det}[M]$ of the matrix M whose entries are $M_{ij} = \langle \phi_j^{(2)} | \phi_i^{(1)} \rangle$. In the following, we shall be mainly interested in the one- and two-body correlation functions of the gas. By making use of the Jacobi theorem [17], these can be usefully rewritten in the following compact forms:

$$\langle \hat{\Psi}_\sigma^\dagger(x) \hat{\Psi}_{\sigma'}(x') \rangle = \text{Det}[M] \sum_{ij} (M^{-1})_{ij} \phi_i^{(2)*}(x, \sigma) \phi_j^{(1)}(x', \sigma') \quad (13)$$

and

$$\begin{aligned} & \left\langle \hat{\Psi}_\sigma^\dagger(x) \hat{\Psi}_\sigma^\dagger(x') \hat{\Psi}_\sigma(x'') \hat{\Psi}_\sigma(x''') \right\rangle = \\ & = \text{Det}[M] \sum_{ijkl} \text{Det} \begin{bmatrix} (M^{-1})_{il} & (M^{-1})_{ik} \\ (M^{-1})_{jl} & (M^{-1})_{jk} \end{bmatrix} \phi_i^{(2)*}(x, \sigma) \phi_j^{(2)*}(x', \sigma') \phi_k^{(1)}(x'', \sigma'') \phi_l^{(1)}(x''', \sigma''') \end{aligned} \quad (14)$$

In a practical simulation, the averages are performed by means of Monte Carlo techniques. A description of the details of the numerical algorithm used is given in Appendix A.

IV. MONTE CARLO RESULTS FOR THE CORRELATION FUNCTIONS

A Monte Carlo code based on the stochastic approach described in the previous section has been used to numerically compute the expectation values of some one- and two-body correlation functions for a one-dimensional Fermi gas with attractive binary interactions as described by the Hamiltonian (1) with $g_0 < 0$. The results of analogous calculations performed with a very similar Monte Carlo algorithm have been reported recently in [18]. Other Quantum Monte Carlo schemes have also been applied to the numerical study of the fermionic Hubbard model with attractive interactions at finite temperature. In particular, the determinantal QMC algorithm [19] has been used to study the correlation functions in 2D [20] and the transition temperature to a pair condensate state in 2D [21, 22] and in 3D [23].

For our simulations, a lattice of $\mathcal{N} = 16$ points was taken, with a total number of $N = 12$ atoms. A number \mathcal{M} of imaginary-time steps comprised between 400 and 1000 has been used. As already mentioned, the ensemble in which observables are calculated is the canonical one; note that the number of particles in each of the spin state can fluctuate, only the total number of particles is fixed. As the two spin components are equivalent, the mean densities in each of the spin components are equal:

$$\rho_\uparrow = \rho_\downarrow = \frac{N}{2L}. \quad (15)$$

The state of the gas in the absence of interactions and at $T = 0$ is depicted in Fig. 1: in a given spin component, the 5 lowest-lying single particle energy levels are totally filled, whereas the two degenerate states of wavevectors $k_+ = k_F = 6\pi/L$ and $k_- = -k_F$ are half-filled. More precisely, 10 atoms are frozen in the states of $|k| < k_F$, and the two remaining atoms are distributed among the 4 degenerate states, $|\uparrow$ or $\downarrow, \pm k_F$, which can be done in 6 different ways. In presence of attractive interactions, this degeneracy will obviously be lifted and the configurations with one atom \uparrow and one atom \downarrow with opposite momenta in the degenerate multiplicity are favorable to the formation of a Cooper pair.

A. One body correlation functions

The simplest observable to compute is the one-body correlation function in a single spin state σ (normalized to the density ρ_σ):

$$g_{\sigma\sigma}^{(1)}(x) = \frac{1}{\rho_\sigma} \langle \hat{\Psi}_\sigma^\dagger(x) \hat{\Psi}_\sigma(0) \rangle. \quad (16)$$

The Monte Carlo prediction is plotted in fig.2 for different values of the temperature: as expected, this correlation function is short-ranged, coherence extending only on a length of the order of the Fermi length $\ell_F = 1/k_F$ for $T < T_F$. This correlation function is indeed the Fourier transform of the momentum distribution of the gas. As the interactions affect the momentum distribution only in a thin region around the Fermi surface (the Fermi points in our one-dimensional geometry), they do not significantly modify its shape as compared to the ideal Fermi distribution.

Because of the rotational symmetry of the density operator in the spin space, the one-body correlation function in different spin states:

$$g_{\uparrow\downarrow}^{(1)}(x) = \frac{1}{\sqrt{\rho_\uparrow\rho_\downarrow}} \langle \hat{\Psi}_\uparrow^\dagger(x) \hat{\Psi}_\downarrow(0) \rangle \quad (17)$$

is instead always identically vanishing.

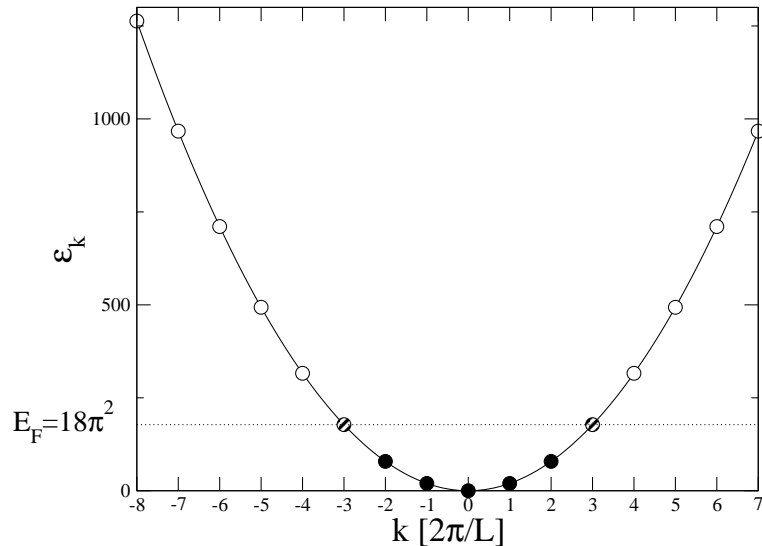


FIG. 1: Schematic view of the state of the ideal Fermi gas at zero temperature for the model considered in the Monte Carlo simulation, that is with $N = 12$ atoms and $\mathcal{N} = 16$ grid points. Each mode is a plane wave with a wavevector $k = 2\pi s/L$ and an energy $\epsilon_k = \hbar^2 k^2/2m$, where the integer s ranges from -8 to 7 . The modes with $|s| \leq 2$ are totally filled, whereas the modes with $|s| = 3$ are half-filled, the higher energy modes being empty. $E_F = \hbar^2 k_F^2/2m$ is the Fermi energy. The energies are here in units of \hbar^2/mL^2 .

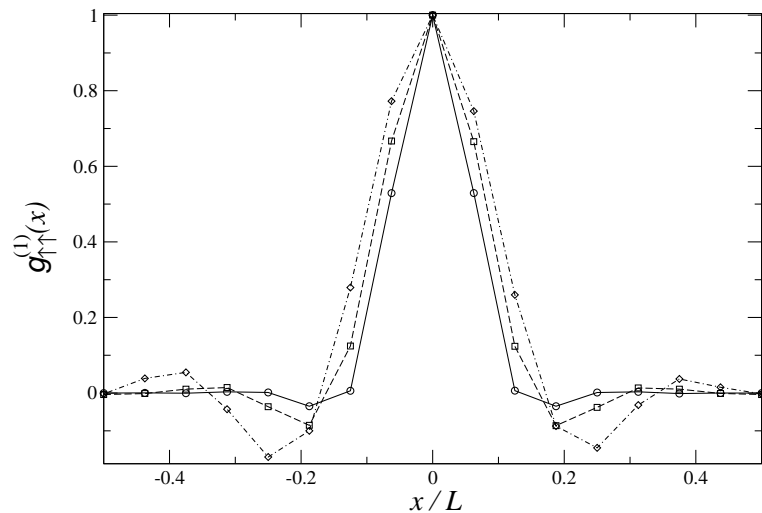


FIG. 2: Single-spin one-body correlation function $g_{\uparrow\uparrow}^{(1)}(x)$ for different values of the temperature $T/T_F = 1.12, 0.56, 0.056$ (circles, squares, diamonds). $N = 12$ atoms on a $\mathcal{N} = 16$ points lattice. Coupling constant $\rho_{\uparrow} g_0/k_B T_F = -0.42$.

B. Density-density correlation functions

Density-density correlation functions are another observable of interest. Both the single-spin density-density correlation function:

$$g_{\sigma\sigma}^{(2)}(x) = \frac{1}{\rho_{\sigma}^2} \langle \hat{\Psi}_{\sigma}^{\dagger}(0) \hat{\Psi}_{\sigma}^{\dagger}(x) \hat{\Psi}_{\sigma}(x) \hat{\Psi}_{\sigma}(0) \rangle = \frac{1}{\rho_{\sigma}^2} \langle \hat{\rho}_{\sigma}(x) \hat{\rho}_{\sigma}(0) \rangle - \frac{1}{\rho_{\sigma}} \delta_{x,0} \quad (18)$$

and the opposite-spin one:

$$g_{\uparrow\downarrow}^{(2)}(x) = \frac{1}{\rho_{\uparrow}\rho_{\downarrow}} \langle \hat{\Psi}_{\uparrow}^{\dagger}(0) \hat{\Psi}_{\downarrow}^{\dagger}(x) \hat{\Psi}_{\downarrow}(x) \hat{\Psi}_{\uparrow}(0) \rangle = \frac{1}{\rho_{\uparrow}\rho_{\downarrow}} \langle \hat{\rho}_{\uparrow}(x) \hat{\rho}_{\downarrow}(0) \rangle, \quad (19)$$

with $\hat{\rho}_\sigma(x) \equiv \hat{\Psi}_\sigma^\dagger(x)\hat{\Psi}_\sigma(x)$, have been calculated by Monte Carlo and plotted as a function of x respectively in fig.3a and in fig.3b. In fig.4, we have plotted $g_{\uparrow\downarrow}^{(2)}(0)$ as a function of temperature. The magnitude of actual density correlations is quantified by the difference $g_{\sigma\sigma'}^{(2)}(x) - 1$.

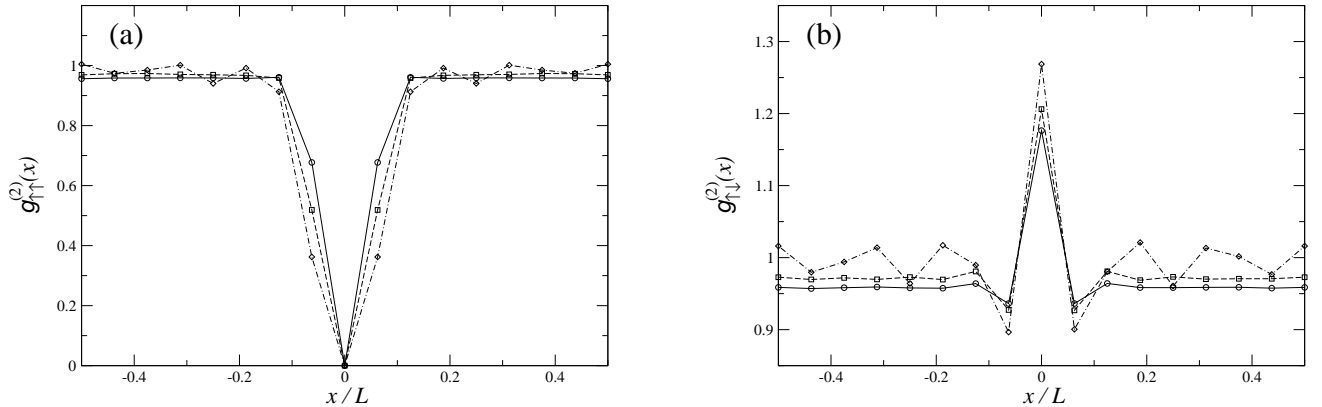


FIG. 3: Single-spin (a) and opposite-spin (b) density-density correlation function $g_{\uparrow\uparrow}^{(2)}(x)$ and $g_{\uparrow\downarrow}^{(2)}(x)$ for different values of the temperature $T/T_F = 1.12, 0.56, 0.056$ (circles, squares, diamonds). Same system parameters as in fig.2.

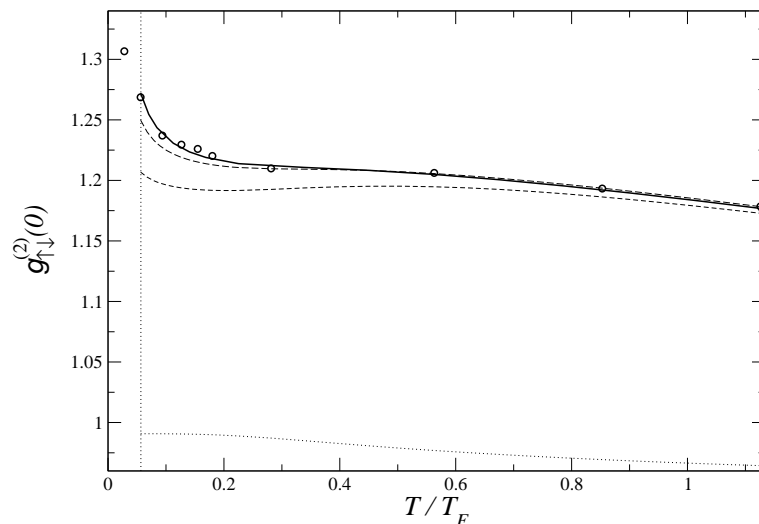


FIG. 4: Opposite spin density-density correlation function at $x = 0$: $g_{\uparrow\downarrow}^{(2)}(0)$ as a function of the temperature T in the canonical ensemble. Circles: Monte Carlo results. Dotted, short dashed, long dashed, solid lines: perturbative results upto order respectively 0, 1, 2, and 3. Same system parameters as in fig.2. The vertical line is the somewhat arbitrary lower bound on the temperature range where perturbation theory converges rapidly.

On one hand, the density correlations in a single spin state described by $g_{\uparrow\uparrow}^{(2)}$ show a short-range hole (Pauli hole) of width similar to the bump of the one-body correlation function $g_{\uparrow\uparrow}^{(1)}$ and are weakly affected by the interactions and by the temperature variations (fig.3a).

On the other hand, the density correlations between opposite spins described by $g_{\uparrow\downarrow}^{(2)}$ show an interesting temperature dependence in the presence of attractive interactions. The lower is the temperature, the most effective are in fact the interactions and therefore the stronger the bunching of opposite spin particles on a given lattice site. In fig.3b we have plotted the spatial profile of $g_{\uparrow\downarrow}^{(2)}(x)$ for different values of the temperature: for the lowest value of T/T_F , notice not only the increase of $g_{\uparrow\downarrow}^{(2)}(0)$, but also the appearance of oscillations as a function of x . As we shall see in the next subsection, at this temperature a condensate of pairs is present. The oscillations then result from the contribution of two distinct effects: the Friedel oscillations in the correlation functions of the normal phase which follow from the

sharpness of the Fermi surface [13], and the oscillations shown by the Cooper pair wavefunction described within the BCS theory by the pairing function $\langle \hat{\Psi}_\uparrow(x)\hat{\Psi}_\downarrow(0) \rangle$. In fig.4 we have summarized the values of $g_{\uparrow\downarrow}^{(2)}(0)$ as a function of the temperature. Notice that $g_{\uparrow\downarrow}^{(2)}(0) - 1$ is appreciable already at the highest temperature considered in fig.4, which, as we shall see in the next subsection, is much higher than the critical temperature T^* for the appearance of long-range order.

C. First-order pair coherence function

It is believed in statistical physics that the superfluid transition in two-component Fermi systems with attractive binary interactions is related to the appearance of long-range order in the so-called *anomalous* averages [10]. In symmetry breaking theories such as the BCS one, this feature corresponds to a non-vanishing value for the gap function defined as:

$$\Delta = -g_0 \langle \hat{\Psi}_\uparrow(x)\hat{\Psi}_\downarrow(x) \rangle, \quad (20)$$

which plays the role of the order parameter of the phase transition in a Ginzburg-Landau approach. In number conserving approaches, quantities like (20) are zero. The phase transition however still appears in the long-range behaviour of correlation functions of the form:

$$g_{\text{pair}}^{(1)}(x) = \frac{1}{\rho_\uparrow \rho_\downarrow} \langle \hat{\Psi}_\downarrow^\dagger(x) \hat{\Psi}_\uparrow^\dagger(x) \hat{\Psi}_\uparrow(0) \hat{\Psi}_\downarrow(0) \rangle. \quad (21)$$

A similar criterion was used in [21, 22, 23] to determine the transition temperature.

A simple physical interpretation of $g_{\text{pair}}^{(1)}$ can be provided as the first order correlation function of pairs: the operator $\hat{\Psi}_\uparrow(0)\hat{\Psi}_\downarrow(0)$ annihilates in fact a pair of particles in opposite spin states at the spatial position 0 and the operator $\hat{\Psi}_\uparrow^\dagger(x)\hat{\Psi}_\downarrow^\dagger(x)$ creates them back at x . This correlation function is therefore formally equivalent to the first order coherence function of a composite boson formed by a pair of fermions with opposite spins. From this point of view, the non-vanishing long-range limit of $g_{\text{pair}}^{(1)}(x)$ is a signature of a quantum condensation of pairs.

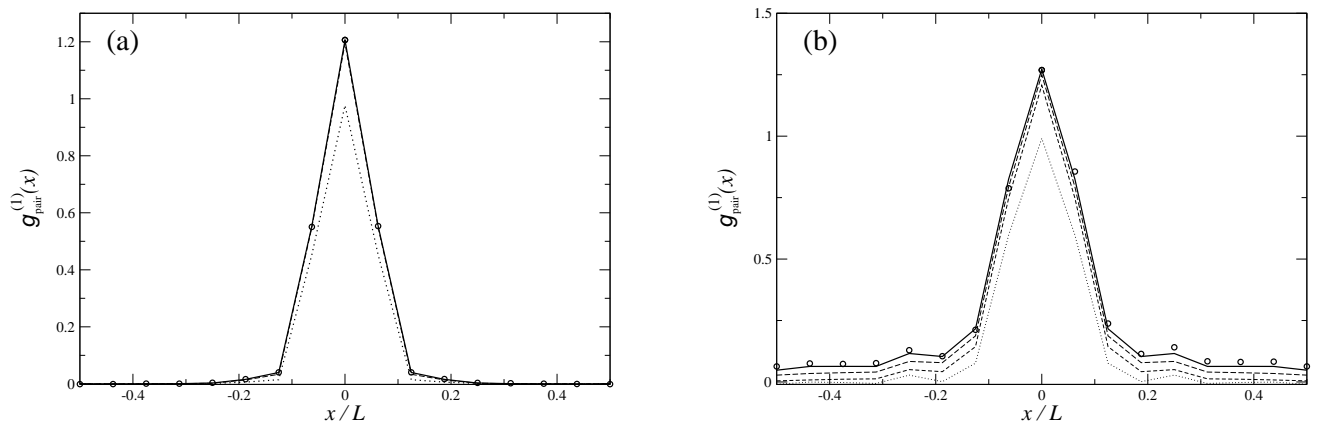


FIG. 5: Normalized pair coherence function $g_{\text{pair}}^{(1)}(x)$ for two different temperatures $T = 0.56T_F$ (left panel) and $T = 0.056T_F$ (right panel) in the canonical ensemble. Circles: Monte Carlo results. Dotted, dashed, solid lines in left panel: perturbative results upto order respectively 0, 1 and 2 (orders 1 and 2 are undistinguishable). Dotted, short dashed, long dashed, solid lines in right panel: perturbative results upto order respectively 0, 1, 2, and 3. Same system parameters as in fig.2.

Monte Carlo simulations for this quantity are shown in fig.5. At low temperatures, $g_{\text{pair}}^{(1)}(x)$ has a finite value also for $x = L/2$, i.e. at the largest distance from 0 allowed by the finite size of the box. On the other hand, at higher temperatures, but still much lower than the Fermi temperature, $g_{\text{pair}}^{(1)}(L/2)$ becomes very small and the long-range order is destroyed. To make this cross-over more apparent, we have plotted in Fig. 6 the value of $g_{\text{pair}}^{(1)}(L/2)$ as a function of the temperature: a sudden rise of this quantity appears at low temperatures. This behavior qualitatively

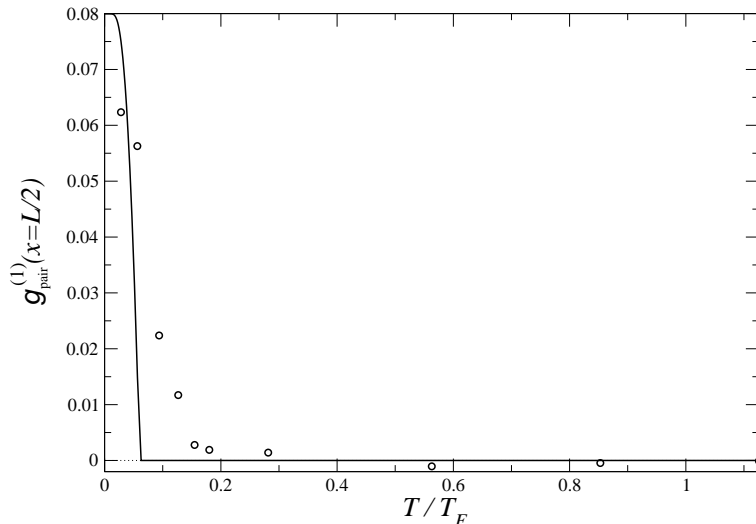


FIG. 6: Pair coherence function $g_{\text{pair}}^{(1)}(L/2)$ as a function of the temperature T . Circles: Monte Carlo results in the canonical ensemble. Solid line: BCS theory. Same system parameters as in fig.2.

corresponds to the one expected for a BCS transition: although a BCS transition can not occur in one dimension in the thermodynamical limit because of long wavelength fluctuations destroying the long range order [24], it can however be observed in our simulations because of the finite size of the system. As the system is finite, the transition temperature T^* is not precisely defined and the long-range order has an analytic dependence on temperature. Notice that the opposite spin density-density correlation described by $g_{\uparrow\downarrow}^{(2)}(0)$ are already important at $T > T^*$ and for $T < T^*$ they only get slightly reinforced.

D. Second-order momentum space correlation function

Another observable that has been recently proposed as a possible way of detecting the transition to a pair condensate state is the second-order momentum space correlation function [25]:

$$G_k^{(2)}(k) = \langle \hat{n}_{k\uparrow} \hat{n}_{-k\downarrow} \rangle - \langle \hat{n}_{k\uparrow} \rangle \langle \hat{n}_{-k\downarrow} \rangle, \quad (22)$$

where the operator $\hat{n}_{k\sigma} = \hat{a}_{k\sigma}^\dagger \hat{a}_{k\sigma}$ gives the occupation of the plane wave k with spin component σ .

As discussed in [25], BCS theory predicts that correlations should be absent above T_{BCS} , that is $G_k^{(2)} = 0$, while the transition to a condensate state should be observable as the appearance of a non-vanishing value of $G_k^{(2)}$, sharply peaked around $k = k_F$.

In fig.7, we have plotted Monte Carlo results for $G_k^{(2)}$ as a function of k for different values of the temperature. At all temperatures, the quantity is indeed strongly peaked at $k = k_F$, and nearly vanishes at the other values. A summary of the temperature-dependence of $G_k^{(2)}(k_F)$ is plotted in fig.8. At temperatures above the transition temperature T^* , correlations are negative and increase as the temperature is lowered. The negative correlation simply follows from the fact that we are working in the canonical ensemble, that is at a fixed total number of particles (see the ideal Fermi gas result in fig.8). As the temperature drops below T^* , the correlations change sign becoming large and positive. This is a signature of pairing: because of the attractive interactions, the states with a filled Fermi sphere plus two particles in states of opposite momenta and spins are in fact energetically favoured. In this state, the fluctuations of the occupation numbers of the k_F, \uparrow and $-k_F, \downarrow$ states are positively correlated.

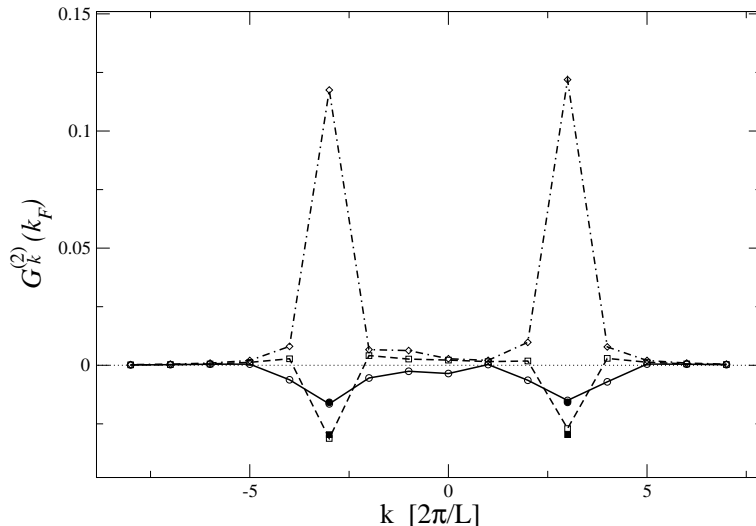


FIG. 7: Second-order momentum space correlation function $G_k^{(2)}(k)$ for different values of the temperature. Empty circles, squares, diamonds: Monte Carlo results for $T/T_F = 0.56, 0.28, 0.056$. Filled circles and squares at $k = \pm k_F$: perturbative expansion up to order 3 for $T/T_F = 0.56, 0.28$ respectively. For $T/T_F = 0.056$ a perturbative expansion to an order higher than 3 would be required to observe convergence.

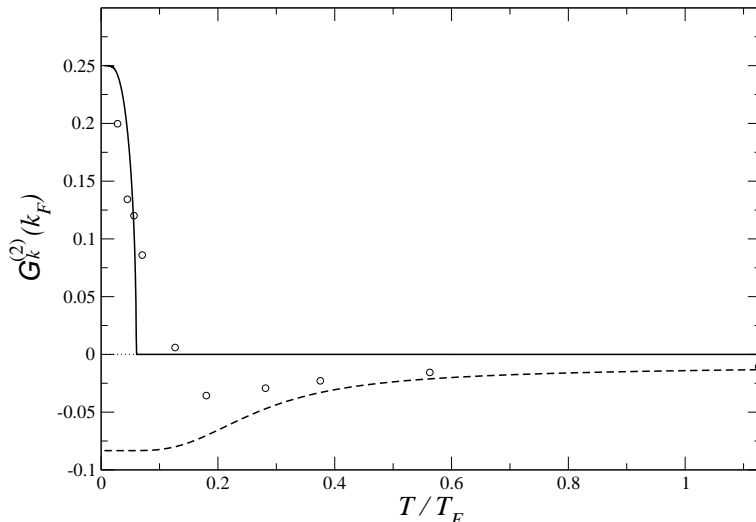


FIG. 8: Second-order momentum space correlation function at $k = k_F$: $G_k^{(2)}(k_F)$ as a function of the temperature T . Circles: Monte Carlo results in the canonical ensemble. Solid line: BCS theory in the grand canonical ensemble. Dashed line: ideal gas in the canonical ensemble. Same system parameters as in fig.2.

V. RESULTS OF A PERTURBATIVE EXPANSION IN g_0

In this section, we explain how to calculate the pair coherence function $g_{\text{pair}}^{(1)}$ and the density correlation function $g_{\uparrow\downarrow}^{(2)}$ by means of a series expansion in powers of the coupling constant g_0 . The same procedure was used in fig.7 to obtain a series expansion for the momentum-space second order correlation function $G_k^{(2)}$ although we do not give here the details of the calculation. We expect this perturbative approach performed around the ideal Fermi gas to be efficient mainly at $T > T^*$ that is in absence of a condensate of pairs. For $T < T^*$ we indeed found numerically that the series (up to order 3) is slowly convergent. Note that such a series expansion can however be shown to be convergent at non-zero temperature for our model system with a finite number of modes, see below.

A. In the canonical ensemble

As we wish to compare to the Quantum Monte Carlo results, we have in principle to perform the perturbative treatment directly in the canonical ensemble with N particles. The resulting averages in the ideal Fermi gas thermal state are however difficult to evaluate analytically. We therefore apply the following trick to ‘canonize’ the grand canonical ensemble. We introduce an unnormalized grand canonical thermal density operator defined as

$$\sigma_{\text{gc}}(\theta) = e^{-\beta(\mathcal{H}-\mu_0\hat{N})}e^{i\theta\hat{N}} \quad (23)$$

where \hat{N} is the total number operator, θ is an angle and μ_0 is the chemical potential of the ideal Fermi gas with an average number of N particles. Taking the Fourier component of $\sigma(\theta)$ over the harmonic $e^{i\theta N}$ amounts to projecting $\sigma(\theta)$ over the subspace with exactly N particles. The canonical expectation value of an operator O is therefore exactly given by [31]:

$$\langle O \rangle_N = \frac{\int_0^{2\pi} d\theta e^{-i\theta N} \text{Tr}[\sigma_{\text{gc}}(\theta)O]}{\int_0^{2\pi} d\theta e^{-i\theta N} \text{Tr}[\sigma_{\text{gc}}(\theta)]}. \quad (24)$$

We then expand $e^{-\beta\mathcal{H}}$ in powers of the interaction potential V , here up to third order:

$$e^{-\beta(\mathcal{H}-\mu_0\hat{N})} = e^{-\beta(\mathcal{H}_0-\mu_0\hat{N})} \left[1 - \int_0^\beta d\tau_1 V(\tau_1) + \int_0^\beta d\tau_2 \int_0^{\tau_2} d\tau_1 V(\tau_2)V(\tau_1) - \int_0^\beta d\tau_3 \int_0^{\tau_3} d\tau_2 \int_0^{\tau_2} d\tau_1 V(\tau_3)V(\tau_2)V(\tau_1) + \dots \right] \quad (25)$$

where \mathcal{H}_0 is the kinetic energy operator of the gas and the imaginary time interaction picture for an operator X is defined as

$$X(\tau) = e^{\tau(\mathcal{H}_0-\mu_0\hat{N})} X e^{-\tau(\mathcal{H}_0-\mu_0\hat{N})}. \quad (26)$$

For a non-zero temperature and a finite number of grid points, the norm of the operator $V(\tau)$ is finite as both V and $\mathcal{H}_0-\mu_0\hat{N}$ have a finite norm. As a consequence, the norm of the n^{th} -order contribution to the series expansion Eq. (25) can be bounded from above by $A^n/n!$ where A is some number, and the series Eq. (25) is absolutely convergent [32].

The calculation of the numerator of Eq. (24) then involves the θ -dependent grand canonical partition function of the ideal Fermi gas and θ -dependent expectation values in the grand canonical ideal Fermi gas:

$$\Xi_0(\theta) \equiv \text{Tr}[\sigma_{\text{gc}}^0(\theta)] = \prod_k \left(1 + e^{-\beta[\hbar^2 k^2/(2m)-\mu_0]} e^{i\theta} \right)^2 \quad (27)$$

$$\langle X \rangle_0(\theta) \equiv \frac{1}{\Xi_0(\theta)} \text{Tr}[\sigma_{\text{gc}}^0(\theta)X] \quad (28)$$

where the square originates from the presence of two spin components. The operator X is one of the terms inside the square brackets of Eq.(25). The expectation values can be evaluated using Wick’s theorem and involve the following particle and hole correlation functions:

$$G_0(x, \tau; \theta) = \langle \hat{\psi}_\uparrow^\dagger(x, \tau) \hat{\psi}_\uparrow(0) \rangle_0(\theta) \quad (29)$$

$$\bar{G}_0(x, \tau; \theta) = \langle \hat{\psi}_\uparrow(x, \tau) \hat{\psi}_\uparrow^\dagger(0) \rangle_0(\theta). \quad (30)$$

The explicit expressions of the relevant expectation values in terms of G_0 and \bar{G}_0 are given in the Appendix B. The integrals over the ‘times’ τ_1, τ_2, τ_3 and the sums over the grid points associated to each factor $V(\tau_i)$ are performed numerically. As each integral is discretized in 256 steps and there are 16 grid points in the lattice, the calculation of the third order correction involves the summation of about 10^{10} terms for a given value of θ .

The perturbative results for the $x = 0$ pair distribution function $g_{\uparrow\downarrow}^{(2)}(0)$ are plotted against the Monte Carlo results as a function of temperature in Fig. 4 for various orders of the perturbative expansion. The agreement with the second order expansion is perfect at high temperature, whereas the third order contribution is required to have agreement

at lower temperatures [33]. For a given temperature, the x dependence of $g_{\uparrow\downarrow}^{(2)}(x)$ predicted by the perturbative expansion is also in good agreement with the exact Monte Carlo results. For $g_{\text{pair}}^{(1)}(x)$, the agreement is also good, at high temperature in Fig. 5a, as well as at a temperature $T < T^*$ in Fig. 5. The fact that the third order prediction is very close to the Quantum Monte Carlo results even when long range order is present may be fortuitous: it significantly differs from the second order prediction so that a calculation of the fourth order correction is required to justify the truncation of the series at this order.

B. In the grand canonical ensemble

It is actually interesting to perform also the perturbative expansion in the grand canonical ensemble: simpler analytical formulas can be obtained, which can be used to test existing approximate theories applicable to the grand canonical ensemble. The unnormalized density operator of the gas is now

$$\sigma_{\text{gc}} = e^{-\beta(\mathcal{H} - \mu\hat{N})}. \quad (31)$$

The perturbative expansion has to be performed for a fixed value of the mean total number of particles equal to N . As a consequence the value of the chemical potential μ is not known in advance and has to be adjusted order by order in the perturbative expansion. To this end, we write

$$\mu = \mu_0 + \delta\mu \quad (32)$$

where μ_0 is the chemical potential of the ideal Fermi gas having on the mean a number N of particles. This amounts to performing the following splitting:

$$\mathcal{H} - \mu\hat{N} = (\mathcal{H}_0 - \mu_0\hat{N}) + W \quad (33)$$

where the perturbation is now

$$W = V - \delta\mu\hat{N}, \quad (34)$$

both terms in W being of order g_0 . We shall restrict here for simplicity to a second order expansion. From Eq.(25) we get

$$\langle O \rangle = \frac{\langle O \rangle_0 - \int_0^\beta d\tau_1 \langle W(\tau_1)O \rangle_0 + \int_0^\beta d\tau_2 \int_0^{\tau_2} d\tau_1 \langle W(\tau_2)W(\tau_1)O \rangle_0 + \dots}{1 - \int_0^\beta d\tau_1 \langle W(\tau_1) \rangle_0 + \int_0^\beta d\tau_2 \int_0^{\tau_2} d\tau_1 \langle W(\tau_2)W(\tau_1) \rangle_0 + \dots} \quad (35)$$

where $\langle X \rangle = \text{Tr}[\sigma_{\text{gc}}X]/\text{Tr}[\sigma_{\text{gc}}]$ stands for the expectation value in the grand canonical density operator of the interacting gas Eq. (31) and $\langle X \rangle_0$ stands for the expectation value in the grand canonical density operator $\exp[-\beta(\mathcal{H}_0 - \mu_0\hat{N})]$ of the ideal Fermi gas. Expanding the inverse of the denominator in Eq.(35) and keeping terms up to second order, one obtains

$$\langle O \rangle = \langle O \rangle_0 - \int_0^\beta d\tau_1 \langle \langle W(\tau_1)O \rangle \rangle_0 + \int_0^\beta d\tau_2 \int_0^{\tau_2} d\tau_1 \langle \langle W(\tau_2)W(\tau_1)O \rangle \rangle_0 + O(g_0^3) \quad (36)$$

where we have introduced the irreducible averages of products of operators A, B, C :

$$\langle \langle AB \rangle \rangle_0 \equiv \langle AB \rangle_0 - \langle A \rangle_0 \langle B \rangle_0 \quad (37)$$

$$\begin{aligned} \langle \langle ABC \rangle \rangle_0 &\equiv \langle ABC \rangle_0 - \langle A \rangle_0 \langle BC \rangle_0 - \langle B \rangle_0 \langle AC \rangle_0 - \langle C \rangle_0 \langle AB \rangle_0 \\ &\quad + 2\langle A \rangle_0 \langle B \rangle_0 \langle C \rangle_0 \end{aligned} \quad (38)$$

and where we used the identity

$$\frac{1}{2} \left(\int_0^\beta d\tau_1 \langle W(\tau_1) \rangle_0 \right)^2 = \int_0^\beta d\tau_2 \int_0^{\tau_2} d\tau_1 \langle W(\tau_2) \rangle_0 \langle W(\tau_1) \rangle_0. \quad (39)$$

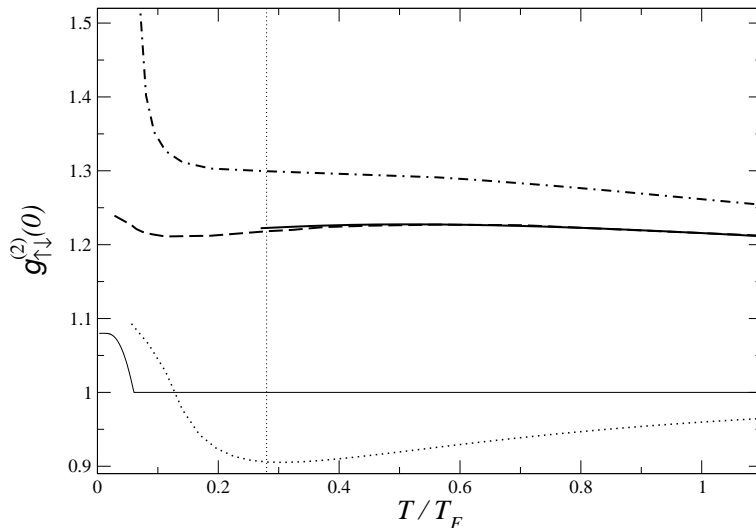


FIG. 9: Opposite spin density-density correlation function at $x = 0$: $g_{\uparrow\downarrow}^{(2)}(0)$ as a function of the temperature T in the grand-canonical ensemble. Solid line: perturbative result at order 2. Dashed line: density-density RPA. Dotted line: Nozières Schmitt-Rink theory. Dot-dashed line: $\Psi^\dagger\Psi^\dagger - \Psi\Psi$ RPA. Thin solid line: BCS theory. The vertical line is an approximate lower bound on T where the second order perturbative theory is accurate; its position was determined by a comparison to the Quantum Monte Carlo results of Fig. 4. Same system parameters as in fig.2. The mean number of particles is fixed to $\langle N \rangle = 12$.

To calculate $\delta\mu$ up to second order, we express the fact that the mean density of spin up particles is fixed in $x = 0$. As the system has translational and spin symmetry, this is equivalent to fixing the mean total number of particles. We therefore specialize Eq.(36) to the case $O = \hat{\psi}_\uparrow^\dagger(0)\hat{\psi}_\uparrow(0)$ and obtain [34]

$$\delta\mu = \frac{1}{2}g_0\rho + g_0^2 \frac{\int_0^\beta d\tau_2 \int_0^{\tau_2} d\tau_1 (dx)^2 \sum_{x_1, x_2} P_{21}H_{21}(P_{21}H_{20}P_{10} - P_{20}H_{21}H_{10})}{\int_0^\beta d\tau_1 dx \sum_{x_1} P_{10}H_{10}} + O(g_0^3) \quad (40)$$

where dx is the spatial step of the grid, ρ is the total density and the following notations were introduced:

$$P_{ij} \equiv \langle \hat{\psi}_\uparrow^\dagger(x_i, \tau_i)\hat{\psi}_\uparrow(x_j, \tau_j) \rangle_0 \quad (41)$$

$$H_{ij} \equiv \langle \hat{\psi}_\uparrow(x_i, \tau_i)\hat{\psi}_\uparrow^\dagger(x_j, \tau_j) \rangle_0 \quad (42)$$

for integers i, j equal to 0, 1 or 2 and with the convention $x_0 = 0, \tau_0 = 0$. Note that the term of order g_0 in $\delta\mu$ coincides with the Hartree-Fock mean field prediction.

In a second step, we calculate $g_{\uparrow\downarrow}^{(2)}(0)$ by taking $O = \hat{\psi}_\uparrow^\dagger(0)\hat{\psi}_\uparrow(0)\hat{\psi}_\downarrow^\dagger(0)\hat{\psi}_\downarrow(0)$. Eliminating $\delta\mu$ from the resulting expression gives:

$$\begin{aligned} (\rho/2)^2 g_{\uparrow\downarrow}^{(2)}(0) &= (\rho/2)^2 - g_0 \int_0^\beta d\tau_1 dx \sum_{x_1} (P_{10}H_{10})^2 \\ &+ g_0^2 \int_0^\beta d\tau_2 \int_0^{\tau_2} d\tau_1 (dx)^2 \sum_{x_1, x_2} (P_{21}H_{20}P_{10} - P_{20}H_{21}H_{10})^2 \\ &+ O(g_0^3). \end{aligned} \quad (43)$$

In the case of a negative coupling constant g_0 , both the first and second order terms are positive, leading to a spatial bunching of opposite spin particles, as expected for attractive interaction.

From the comparison with the quantum Monte Carlo calculations in the canonical ensemble, we know the temperature range over which the second order perturbative expansion gives accurate predictions for $g_{\uparrow\downarrow}^{(2)}(0)$. For the grand canonical ensemble with the same mean number of particles, we expect the same conclusion to apply. We therefore

use a numerical integration of Eq.(43) as a test of existing approximate theories that will be reviewed in sec.VI. As is apparent in Fig. 9, the density-density RPA is in very good agreement with the perturbative result, whereas the $\Psi^\dagger\Psi^\dagger - \Psi\Psi$ RPA overestimates $g_{\uparrow\downarrow}^{(2)}(0)$ and the Nozières-Schmitt-Rink prediction clearly underestimates it. At temperatures above the BCS critical temperature, the BCS theory reduces to the mean-field Hartree-Fock theory which gives for $g_{\uparrow\downarrow}^{(2)}(0)$ simply the ideal Fermi gas result, $g_{\uparrow\downarrow}^{(2)}(0) = 1$.

VI. COMPARISON WITH APPROXIMATE THEORIES

For the grand canonical ensemble, several approximate many-body theories exist which can be used to obtain predictions for the correlation functions of the interacting Fermi gas. In the next subsections, some among the most famous ones are discussed, namely the mean-field BCS theory [10, 11], two versions of the random-phase approximation (RPA) [12, 13], and the Nozières-Schmitt Rink (NSR) theory [6] developed to study the BCS-BEC crossover in strongly interacting gases. A quantitative comparison with the prediction of a grand canonical version of the perturbative expansion of section V will be performed. In order for the comparison to be meaningful, the many-body theories under investigation have been specialized to the specific case of the discrete lattice Hamiltonian (1) with exactly the same discretization parameters as used in the previous sections.

A. BCS theory

In the BCS theory, the equilibrium density matrix is determined in a self-consistent way from the mean-field quadratic Hamiltonian of the grand canonical ensemble at a chemical potential μ :

$$\mathcal{H}_{\text{BCS}} = \sum_{k\sigma} \left(\frac{\hbar^2 k^2}{2m} - \mu \right) \hat{a}_{k\sigma}^\dagger \hat{a}_{k\sigma} + g_0 \sum_{x\sigma} dx \rho_{-\sigma} \hat{\Psi}_\sigma^\dagger(x) \hat{\Psi}_\sigma(x) - \sum_x (\hat{\Psi}_\uparrow(x) \hat{\Psi}_\downarrow(x) \Delta^* + \hat{\Psi}_\downarrow^\dagger(x) \hat{\Psi}_\uparrow^\dagger(x) \Delta) \quad (44)$$

where the mean density ρ_σ in a given spin component and the gap function Δ are defined as usual as:

$$\rho_\sigma = \langle \hat{\Psi}_\sigma^\dagger(x) \hat{\Psi}_\sigma(x) \rangle \quad (45)$$

$$\Delta = -g_0 \langle \hat{\Psi}_\uparrow(x) \hat{\Psi}_\downarrow(x) \rangle. \quad (46)$$

The quadratic Hamiltonian (44) is easily diagonalized by a Bogoliubov transformation in the plane wave basis:

$$\mathcal{H}_{\text{BCS}} = \sum_{k\sigma} E_k \hat{c}_{k\sigma}^\dagger \hat{c}_{k\sigma}, \quad (47)$$

where the \hat{c} , \hat{c}^\dagger operators satisfy Fermi anticommutation rules and are related to the Fermi field operators by:

$$\hat{\Psi}_\downarrow(x) = \frac{1}{\sqrt{L}} \sum_k u_k e^{ikx} \hat{c}_{k\downarrow} + v_k e^{ikx} \hat{c}_{-k,\uparrow}^\dagger \quad (48)$$

$$\hat{\Psi}_\uparrow(x) = \frac{1}{\sqrt{L}} \sum_k u_k e^{ikx} \hat{c}_{k\uparrow} - v_k e^{ikx} \hat{c}_{-k\downarrow}^\dagger \quad (49)$$

where the positive coefficients u_k , v_k of the Bogoliubov transformation are defined by:

$$u_k^2 = 1 - v_k^2 = \frac{1}{2} \left(1 + \frac{\frac{\hbar^2 k^2}{2m} - \tilde{\mu}}{E_k} \right), \quad (50)$$

the quasi-particle energies E_k are given by:

$$E_k = \sqrt{\Delta^2 + \left(\frac{\hbar^2 k^2}{2m} - \tilde{\mu} \right)^2} \quad (51)$$

and the chemical potential is shifted as $\tilde{\mu} = \mu - g_0 \rho_\sigma$ so as to take into account the mean-field energy. The self-consistency equation for the gap Δ is:

$$-\frac{g_0}{2L} \sum_k \frac{1 - 2f_k}{E_k} = 1, \quad (52)$$

where the f_k are the quasi-particle occupation numbers $f_k = (e^{E_k/k_B T} + 1)^{-1}$. For high temperature $T > T_{\text{BCS}}$, Eq.(52) has no solution, so that the system is in the *normal* phase $\Delta = 0$ and the BCS theory reduces to a Hartree-Fock theory. At low temperature $T < T_{\text{BCS}}$, the gap equation is solved for a non-vanishing value of Δ . This value grows as the temperature decreases.

1. Calculation of correlation functions within the BCS theory

The expansion of the field operator (49) in terms of quasi-particle creation and destruction operators can be used to obtain a prediction for the correlation functions. For instance, the BCS prediction for the one-body correlation function $g_{\sigma\sigma}^{(1)}(x)$ is given by:

$$g_{\sigma\sigma}^{(1)}(x) = \frac{1}{\rho_\sigma} \sum_k \frac{e^{-ikx}}{L} [|u_k|^2 f_k + |v_k|^2 (1 - f_k)]. \quad (53)$$

From Wick's theorem, the single-spin density-density correlation function $g_{\sigma\sigma}^{(2)}(x)$ is

$$g_{\sigma\sigma}^{(2)}(x) = 1 - |g_{\sigma\sigma}^{(1)}(x)|^2. \quad (54)$$

Both quantities are affected in a weak way by the attractive interactions and eventually by the appearance of a non-vanishing gap Δ .

A richer physics can be found in the opposite spin density-density correlation function $g_{\uparrow\downarrow}^{(2)}(x)$. For this quantity, the BCS theory predicts:

$$g_{\uparrow\downarrow}^{(2)}(x) = 1 + \frac{1}{\rho_\uparrow \rho_\downarrow} |A(x)|^2, \quad (55)$$

where the anomalous correlation function $A(x)$ is defined as:

$$A(x) = \langle \hat{\Psi}_\downarrow(x) \hat{\Psi}_\uparrow(0) \rangle = \sum_k \frac{e^{ikx}}{L} u_k v_k (1 - 2f_k). \quad (56)$$

As $\Delta = -g_0 A(0)$, $g_{\uparrow\downarrow}^{(2)}(0)$ has the simple expression:

$$g_{\uparrow\downarrow}^{(2)}(0) = 1 + \left| \frac{\Delta}{g_0 \rho_\sigma} \right|^2. \quad (57)$$

For $T > T_{\text{BCS}}$, this quantity is identically 1, which means that the BCS theory does not predict any correlation between the densities in opposite spin states. These appear only for $T < T_{\text{BCS}}$ as a consequence of the non-vanishing BCS gap. As one can see in fig.9, this result is in qualitative disagreement with the perturbative expansion which gives a significant degree of correlation also for $T \simeq T_F \gg T_{\text{BCS}}$.

The BCS prediction for the first-order pair coherence function $g_{\text{pair}}^{(1)}(x)$ is:

$$g_{\text{pair}}^{(1)}(x) = \frac{1}{\rho_\uparrow \rho_\downarrow g_0^2} |\Delta|^2 + g_{\sigma\sigma}^{(1)}(x)^2 \quad (58)$$

and is characterized by a short-ranged bump of spatial size of the order of $\ell_F = 1/k_F$, and a non-vanishing long-range limit. As one can see in fig.6, the long distance behaviour of $g_{\text{pair}}^{(1)}$ predicted by the BCS theory is in qualitative agreement with the Monte Carlo predictions.

B. Random Phase Approximation

1. Fluctuation-dissipation theorem

A simple way of including the fluctuations around the mean-field is to compute a response function within the mean-field theory and then invoke the fluctuation-dissipation theory to obtain the corresponding correlation function. In this subsection, we shall give a short review of the main results of linear response theory that are required to obtain the correlation functions of our interacting Fermi gas. A complete discussion of linear response theory and fluctuation-dissipation theorem can be found in [10, 26].

Let A and B be two operators of a system characterized by a time-independent Hamiltonian \mathcal{H} . For notational simplicity, we assume that at equilibrium $\langle A \rangle_{\text{eq}} = \langle B \rangle_{\text{eq}} = 0$. A weak perturbation of the form:

$$\mathcal{H}_{\text{pert}} = \epsilon(t) A^\dagger + \epsilon^*(t) A \quad (59)$$

is applied to the system and its effect on the observable B recorded. At linear regime, this is summarized by the linear response functions:

$$\langle B \rangle(t) = \int_{-\infty}^{\infty} dt' \left[\chi_{BA}(t-t') \epsilon^*(t') + \chi_{BA^\dagger}(t-t') \epsilon(t') \right]. \quad (60)$$

The linear susceptibilities χ have the simple expression in terms of commutators:

$$\chi_{BA}(t) = \frac{1}{i\hbar} \text{Tr} \left\{ [B(t), A] \rho_{\text{eq}} \right\} \Theta(t), \quad (61)$$

where $\rho_{\text{eq}} = \frac{1}{\mathcal{Z}} e^{-\beta \mathcal{H}}$ is the thermal equilibrium density matrix at $\beta = 1/k_B T$, $\mathcal{Z} = \text{Tr}[e^{-\beta \mathcal{H}}]$ is the partition function and $B(t) = e^{i\mathcal{H}t/\hbar} B e^{-i\mathcal{H}t/\hbar}$. As the Hamiltonian of the unperturbed system does not depend on time, the Fourier transform of $\chi_{BA}(t)$ is the frequency-dependent response function to a harmonic perturbation of frequency ω :

$$\tilde{\chi}_{BA}(\omega) = \int_{-\infty}^{\infty} dt e^{i\omega t} \chi_{BA}(t) e^{-\eta t}, \quad (62)$$

where $\eta \rightarrow 0^+$ [35] The correlation function $\tilde{S}_{BA}(\omega)$ is defined as:

$$\tilde{S}_{BA}(\omega) = \int_{-\infty}^{\infty} dt e^{i\omega t} S_{BA}(t) = \int_{-\infty}^{\infty} dt e^{i\omega t} \langle B(t) A(0) \rangle. \quad (63)$$

If the condition:

$$\text{Tr}[\mathcal{P}_{E_n} B \mathcal{P}_{E_m} A \mathcal{P}_{E_n}] \in \mathbb{R}, \quad (64)$$

holds for all the eigenenergies E_n and E_m of the Hamiltonian \mathcal{H} where the projector \mathcal{P}_E projects onto the eigenspace of energy E , then the fluctuation-dissipation theorem holds in its most common form (Callen-Welton theorem) relating the imaginary part of the response function $\text{Im}[\tilde{\chi}_{BA}(\omega)]$ to the correlation function $\tilde{S}_{BA}(\omega)$:

$$\text{Im}[\tilde{\chi}_{BA}(\omega)] = -\frac{1}{2\hbar} \tilde{S}_{BA}(\omega) (1 - e^{-\beta \hbar \omega}). \quad (65)$$

It is easy to verify that the condition (64) is verified if $A^\dagger = B$ or, more generally, if $A^\dagger = S B S$, S being an arbitrary unitary operator such that $S^2 = 1$.

The fluctuation-dissipation theorem (65) implies that the correlation function $\tilde{S}_{BA}(\omega)$ is fixed by the knowledge of $\text{Im}[\tilde{\chi}_{BA}(\omega)]$ modulo a delta distribution in $\omega = 0$:

$$\tilde{S}_{BA}(\omega) = -2\hbar \frac{\text{Im}[\tilde{\chi}_{BA}(\omega)]}{1 - e^{-\beta \hbar \omega}} + 2\pi C_{BA} \delta(\omega). \quad (66)$$

The constant C_{BA} can be written as follows:

$$C_{BA} = -k_B T \left[\chi_{BA}^{\text{therm}} - \lim_{\omega \rightarrow 0} \tilde{\chi}_{BA}(\omega) \right] \quad (67)$$

in terms of the thermodynamic (isothermal) susceptibility χ_{BA}^{therm} . As usual in thermodynamics, this is defined as the response on B when the system is at thermal equilibrium in the presence of a weak and time-independent perturbation $\mathcal{H}_{\text{pert}} = \epsilon^* A + \epsilon A^\dagger$:

$$\delta B^{\text{therm}} = \epsilon^* \chi_{BA}^{\text{therm}} + \epsilon \chi_{BA^\dagger}^{\text{therm}} \quad (68)$$

resulting from the expansion to first order in ϵ of:

$$\delta B^{\text{therm}} = \frac{\text{Tr}[B e^{-\beta(\mathcal{H} + \epsilon^* A + \epsilon A^\dagger)}]}{\text{Tr}[e^{-\beta(\mathcal{H} + \epsilon^* A + \epsilon A^\dagger)}]}. \quad (69)$$

Notice that while the definition of χ_{BA}^{therm} involves some implicit coupling to a thermal reservoir at temperature T , $\tilde{\chi}_{BA}(\omega)$ is defined for an isolated system evolving under the Hamiltonian \mathcal{H} . For this reason, the thermodynamical susceptibility χ_{BA}^{therm} and the static limit $\tilde{\chi}_{BA}(\omega \rightarrow 0)$ in general are not equal [26].

From the microscopic expression of C_{BA} in terms of the eigenstates of \mathcal{H} of energy E_n :

$$C_{BA} = -\frac{\beta}{Z} \sum_n e^{-\beta E_n} \text{Tr}[\mathcal{P}_n B \mathcal{P}_n A \mathcal{P}_n], \quad (70)$$

one concludes that C_{BA} is not vanishing in the presence of degeneracies between the eigenenergies of \mathcal{H} or when the diagonal matrix elements $\langle n | A | n \rangle$ and $\langle n | B | n \rangle$ are not vanishing.

The possibility of having a term in $\delta(\omega)$ in the correlation function S_{BA} is often neglected in statistical mechanics textbooks, e.g. [10]. Although this is generally correct in the thermodynamical limit, it may lead to incorrect results for the correlation functions of finite systems. Examples of this issue are discussed in the next section and in the Appendix C.

2. Density-density RPA

A prediction for the density-density correlation function of the Fermi gas in the grand canonical ensemble can be obtained by applying the general results of the previous subsection to the operator $\hat{\rho}_\sigma(x)$ giving the particle density in the spin state σ at position x . An approximate prediction for the density-density response functions can be obtained by linearizing the equations of the mean-field theory discussed around the thermal equilibrium state. For historical reasons, this approximation scheme is usually called *random phase approximation* (RPA) [12, 13]. For the sake of simplicity, we shall limit ourselves to the case $T > T_{\text{BCS}}$, regime in which the vanishing of the anomalous averages considerably improves the physical transparency of the formulas.

As the system is spatially homogeneous with the same density ρ_σ in each spin-component, the different Fourier components of the spatial density

$$\delta \hat{\rho}_{k\sigma} = \frac{1}{\sqrt{L}} \sum_x dx e^{-ikx} (\hat{\rho}_\sigma(x) - \rho_\sigma) = \frac{1}{\sqrt{L}} \sum_x dx e^{-ikx} (\hat{\Psi}_\sigma^\dagger(x) \hat{\Psi}_\sigma(x) - \rho_\sigma) \quad (71)$$

are decoupled. Taking $A = \delta \hat{\rho}_{k\sigma}$ and $B = \delta \hat{\rho}_{k'\sigma'}$, the frequency-dependent susceptibility matrix has the form:

$$\tilde{\chi}_{\sigma\sigma'}(k, k'; \omega) = \tilde{\chi}_{\sigma\sigma'}(k, \omega) \delta_{k, k'}. \quad (72)$$

Because of the symmetry in the spin space, $\tilde{\chi}_{\uparrow\uparrow} = \tilde{\chi}_{\downarrow\downarrow}$ and $\tilde{\chi}_{\uparrow\downarrow} = \tilde{\chi}_{\downarrow\uparrow}$, so that the eigenvectors of the susceptibility matrix are the symmetric and antisymmetric linear combination of the two spin states. The corresponding eigenvalues are:

$$\tilde{\chi}_\pm(k, \omega) = \tilde{\chi}_{\uparrow\uparrow}(k, \omega) \pm \tilde{\chi}_{\uparrow\downarrow}(k, \omega). \quad (73)$$

Conversely, the susceptibility matrix $\tilde{\chi}_{\sigma\sigma'}$ in the $\sigma = \uparrow\downarrow$ basis is written as a function of the $\tilde{\chi}_\pm$ as:

$$\tilde{\chi}_{\sigma\sigma'} = \frac{1}{2} \begin{pmatrix} \tilde{\chi}_+ + \tilde{\chi}_- & \tilde{\chi}_+ - \tilde{\chi}_- \\ \tilde{\chi}_+ - \tilde{\chi}_- & \tilde{\chi}_+ + \tilde{\chi}_- \end{pmatrix} \quad (74)$$

The RPA susceptibility of an interacting gas can be calculated from the Hartree-Fock equation of motion [27], and has the simple expression:

$$\tilde{\chi}_{\pm}(k, \omega) = \frac{\tilde{\chi}_0(k, \omega)}{1 \mp g_0 \tilde{\chi}_0(k, \omega)}, \quad (75)$$

in terms of the susceptibility $\tilde{\chi}_0$ of a non-interacting, one component Fermi gas at the same temperature and chemical potential:

$$\tilde{\chi}_0(k, \omega) = \frac{1}{L} \sum_q \frac{f_q - f_{q+k}}{\hbar\omega + \mathcal{E}_q - \mathcal{E}_{q+k} + i0^+}. \quad (76)$$

$\mathcal{E}_q = \hbar^2 q^2 / 2m$ are the energies of the single-particle states and $f_q = (1 + \exp[\beta(\mathcal{E}_q - \mu)])^{-1}$ the corresponding Fermi occupation factors. Notice that the quantity inside the sum vanishes for the states q such that $\mathcal{E}_q = \mathcal{E}_{q+k}$.

An expression analogous to (75):

$$\chi_{\pm}^{\text{therm}}(k) = \frac{\chi_0^{\text{therm}}(k)}{1 \mp g_0 \chi_0^{\text{therm}}(k)}, \quad (77)$$

relates the thermodynamic susceptibilities $\chi_{\pm}^{\text{therm}}(k)$ of the interacting gas to the thermodynamic susceptibility of the non-interacting one-component gas:

$$\chi_0^{\text{therm}}(k) = -\frac{1}{L} \sum_q f_q (1 - f_{q+k}) \cdot \begin{cases} \frac{e^{\beta(\mathcal{E}_q - \mathcal{E}_{q+k})} - 1}{\mathcal{E}_q - \mathcal{E}_{q+k}} & \text{if } \mathcal{E}_q \neq \mathcal{E}_{q+k} \\ \beta & \text{if } \mathcal{E}_q = \mathcal{E}_{q+k} \end{cases} \quad (78)$$

By applying the fluctuation-dissipation theorem in its form (66) to the operators $B = \delta\hat{\rho}_{k\sigma}^{\dagger}$ and $A = \delta\hat{\rho}_{k\sigma'}$, one can write the correlation function

$$S_{\sigma\sigma'}(k, \omega) = \int_{-\infty}^{\infty} dt e^{i\omega t} \langle \delta\hat{\rho}_{k\sigma}^{\dagger}(t) \delta\hat{\rho}_{k\sigma'}(0) \rangle \quad (79)$$

in terms of the imaginary part of $\tilde{\chi}_{\sigma\sigma'}(k, \omega)$ and the thermodynamic susceptibility $\chi_{\sigma\sigma'}^{\text{therm}}(k)$:

$$S_{\sigma\sigma'}(k, \omega) = -2\hbar \frac{\text{Im}[\tilde{\chi}_{\sigma\sigma'}(k, \omega)]}{1 - e^{-\beta\hbar\omega}} - 2\pi k_B T [\chi_{\sigma\sigma'}^{\text{therm}}(k) - \lim_{\omega \rightarrow 0} \tilde{\chi}_{\sigma\sigma'}(k, \omega)] \delta(\omega). \quad (80)$$

The condition (64) is here satisfied since A and B are connected by $B^{\dagger} = SAS$ with S respectively equal to the identity, if $\sigma = \sigma'$, or the spin-inversion operator S exchanging the spin components \uparrow, \downarrow of all the particles, if $\sigma = -\sigma'$.

Finally, the RPA prediction for the desired real-space, one-time density-density correlation function can be found by inverse Fourier transform of $S_{\sigma\sigma'}(k, \omega)$:

$$\langle \hat{\rho}_{\sigma}(x) \hat{\rho}_{\sigma'}(0) \rangle = \rho_{\sigma} \rho_{\sigma'} + \frac{1}{L} \int_{-\infty}^{\infty} \frac{d\omega}{2\pi} \sum_k e^{-ikx} S_{\sigma\sigma'}(k, \omega). \quad (81)$$

Corresponding predictions for the opposite spin density-density correlation function at $x = 0$ as a function of the temperature are plotted in fig.9. Notice the excellent agreement of the RPA prediction with the one of the perturbative expansion in g_0 discussed in sec.V. In our finite system, the agreement strongly relies on the correct inclusion of the $\delta(\omega)$ term in (80). An explicit calculation of this issue for the non-interacting case is presented in the Appendix C.

3. $\Psi^{\dagger}\Psi^{\dagger}\text{-}\Psi\Psi$ RPA

In the previous subsection, we have obtained a prediction for the density-density correlation function $g_{\sigma\sigma'}^{(2)}(x)$ of an interacting Fermi gas by using the RPA density-density susceptibility and then invoking the fluctuation-dissipation

theorem. In the present subsection, a similar approach is used to obtain the pair coherence function $g_{\text{pair}}^{(1)}(x)$ at temperatures higher than the BCS critical temperature T_{BCS} in the grand canonical ensemble.

Consider the pair of operators:

$$B = \hat{\Psi}_{\downarrow}^{\dagger}(x)\hat{\Psi}_{\uparrow}^{\dagger}(x) \quad (82)$$

$$A = \hat{\Psi}_{\uparrow}(0)\hat{\Psi}_{\downarrow}(0). \quad (83)$$

At thermal equilibrium both of them have a vanishing expectation value. The correlation function:

$$\langle BA \rangle = \left\langle \hat{\Psi}_{\downarrow}^{\dagger}(x)\hat{\Psi}_{\uparrow}^{\dagger}(x)\hat{\Psi}_{\uparrow}(0)\hat{\Psi}_{\downarrow}(0) \right\rangle = \rho_{\uparrow}\rho_{\downarrow}g_{\text{pair}}^{(1)}(x) \quad (84)$$

can be evaluated from the susceptibility χ_{BA} .

As in the previous subsection, we introduce the spatial Fourier components as:

$$A_k = \frac{1}{\sqrt{L}} \sum_x dx e^{-ikx} \hat{\Psi}_{\uparrow}(x)\hat{\Psi}_{\downarrow}(x) \quad (85)$$

$$B_k = \frac{1}{\sqrt{L}} \sum_x dx e^{ikx} \hat{\Psi}_{\downarrow}^{\dagger}(x)\hat{\Psi}_{\uparrow}^{\dagger}(x); \quad (86)$$

note the sign difference in the phase factors of (85) and (86). Thanks to the spatial homogeneity of the system, the susceptibility is diagonal in k -space. From the Hartree-Fock-Bogoliubov equation of motion for the anomalous averages [27], one can obtain the following simple expression for the RPA susceptibility:

$$\tilde{\chi}(k, \omega) = \frac{\tilde{\chi}_0(k, \omega)}{1 - g_0 \tilde{\chi}_0(k, \omega)}, \quad (87)$$

where $\tilde{\chi}_0$ is defined as:

$$\tilde{\chi}_0(k, \omega) = \frac{1}{L} \sum_q \frac{2f_q - 1}{\omega + \mathcal{E}_q + \mathcal{E}_{q+k} + g_0\rho - 2\mu + i0^+} \quad (88)$$

and describes the ideal gas response. As previously, \mathcal{E}_q are the energies of the single-particle states, f_q the Fermi occupation factors, and $\rho = \rho_{\uparrow} + \rho_{\downarrow}$ the total particle density summed over both spin states. Notice how $\chi(k=0, \omega=0)$ diverges when $\tilde{\chi}_0(k=0, \omega=0)$ tends to $1/g_0$. This is the signature of the approaching of the BCS transition: the standard equation [10] for the BCS critical temperature is in fact recovered if one imposes:

$$1 = g_0 \chi_0(k=0, \omega=0) = -\frac{g_0}{2L} \sum_q \frac{1 - 2f_q}{\mathcal{E}_q + \frac{1}{2}g_0n - \mu}. \quad (89)$$

As the chemical potential is a variable that can be continuously varied, all degeneracies between states with different particle number are accidental and occur only for discrete values of μ . As A and B have vanishing diagonal elements, the correction term in $\delta(\omega)$ vanishes for all other values of μ . As $g_{\text{pair}}^{(1)}$ has a continuous dependance on μ , there is no need for calculating $\chi^{\text{therm}}(k)$. We therefore have:

$$S_{BA}(k, \omega) = -2\hbar \frac{\text{Im}[\tilde{\chi}(k, \omega)]}{1 - e^{-\beta\hbar\omega}} \quad (90)$$

and

$$g_{\text{pair}}^{(1)}(x) = \frac{1}{\rho_{\uparrow}\rho_{\downarrow}L} \int_{-\infty}^{\infty} \frac{d\omega}{2\pi} \sum_k e^{-ikx} S_{BA}(k, \omega). \quad (91)$$

The condition (64) is here satisfied as $B_k^{\dagger} = A_k$. As $g_{\text{pair}}^{(1)}(x=0)$ coincides with $g_{\uparrow\downarrow}^{(2)}(x=0)$, we have included in fig.9 also the prediction of the present $\Psi^{\dagger}\Psi^{\dagger} - \Psi\Psi$ RPA approach. The agreement with the perturbative expansion is less good than in the case of the density-density RPA approach.

C. Nozières-Schmitt Rink approach

In [6], a non-perturbative calculation is performed for the grand potential of a two component Fermi gas with attractive interactions by a resummation of a certain class of diagrams.

Starting from Eq. (20) of [6] which gives the grand potential Ω in terms of an integral in the complex plane, we can deform the integration contour and apply the residues formula to obtain the following expression in terms of a sum for the case of a contact interaction potential [36]:

$$\Omega(\mu, T; g_0) = \Omega_0(\mu, T) + k_B T \sum_{q, \omega_\nu} \log[1 - \chi(q, \omega_\nu; g_0)] - \frac{g_0}{2L} \sum_{k_1, k_2} (1 - f_{k_1} - f_{k_2}), \quad (92)$$

where $\omega_\nu = 2i\pi\nu/\beta$ with ν integer ranging from $-\infty$ to $+\infty$. The function χ is defined as:

$$\chi(q, \omega; g_0) = -\frac{g_0}{L} \sum_k \frac{1 - f_k - f_{k+q}}{\mathcal{E}_k + \mathcal{E}_{k+q} - 2\mu - \omega}, \quad (93)$$

f_q being the occupation number $f_q = \{1 + \exp[\beta(\mathcal{E}_q - \mu)]\}^{-1}$ and Ω_0 being the grand potential for the ideal two-component Fermi gas.

This theory requires a self-consistent determination of μ from $N = -\partial_\mu \Omega$, which we perform numerically. It gives access to $g_{\uparrow\downarrow}^{(2)}(0)$ thanks to the Hellmann-Feynman theorem [28]:

$$\left(\frac{\rho}{2}\right)^2 g_{\uparrow\downarrow}^{(2)}(0) = \frac{1}{L} \frac{\partial}{\partial g_0} \Omega. \quad (94)$$

The results are plotted in Fig.9. The poor agreement with the perturbative expansion can be explained as follows. Let us expand Eq.(92) upto second order in g_0 at a given μ . If one then replaces μ by its value in the NSR theory for the density under consideration, one gets from Eq.(94) a prediction for $g_{\uparrow\downarrow}^{(2)}(0)$ upto first order that can be compared to the exact expansion Eq.(43):

$$g_{NSR}^{(2)}(0) - g_{\uparrow\downarrow}^{(2)}(0) = \frac{\rho_0^2(\mu_{NSR})}{\rho^2} - 1 + O(g_0^2) \quad (95)$$

Here $\rho_0(\mu)$ is the total density of the ideal two-component Fermi gas for the chemical potential μ . A first order expansion of Ω is enough to obtain the chemical potential $\mu_{NSR} = \mu_0 + g_0\rho/2 + O(g_0^2)$ in the NSR theory and to conclude that $g_{NSR}^{(2)}$ differs from the exact value by a term of the order of g_0 which has the same sign as g_0 . This is just because not all the second order diagrams for Ω have been included in the resummation procedure [37].

VII. CONCLUSIONS

In the present paper, we have presented the result of extensive Quantum Monte Carlo simulations for the static correlation functions of a one-dimensional lattice model of attractively interacting two component fermions. The numerical results obtained by QMC have been compared to existing approximate theories. Excellent agreement with the predictions of a perturbative expansion in the interaction constant has been found, as well as with the ones of the random phase approximation.

Although long-range order is destroyed by phase fluctuations in one-dimensional systems in the thermodynamical limit, the finite size of the system under consideration still allows for the identification of a crossover to a condensed state at the temperature T^* at which the first order coherence length of the pairs becomes larger than the system size.

We have found that a significant degree of opposite spin density-density correlations already exists at temperatures well above T^* and is only slightly enhanced as the temperature goes below T^* . This means that a measurement of the density-density correlation function $g_{\uparrow\downarrow}^{(2)}$ can not provide an unambiguous signature of the onset of a condensed state in the gas. On the other hand, this could be provided by a measurement of the second-order momentum space correlation function as suggested in [25], or, even more directly, of the long-range behaviour of the first-order pair

coherence function $g_{\text{pair}}^{(1)}(x)$. A non-vanishing limit of $g_{\text{pair}}^{(1)}(x)$ for large x corresponds in fact to the presence of a finite condensate fraction in both weak- (BCS) and strong- (BEC) interaction regimes. A possible experimental scheme to measure $g_{\text{pair}}^{(1)}$ in atomic Fermi systems by means of matter-wave interferometric techniques will be the subject of a forthcoming publication.

Acknowledgments

Laboratoire Kastler Brossel is a Unité de Recherche de l'École Normale Supérieure et de l'Université Paris 6, associée au CNRS. We acknowledge discussions with Ph. Chomaz, J. Dalibard, B. Derrida, T. Jolicœur, O. Juillet, A. Montina, C. Mora, A. Recati.

APPENDIX A: THE MONTE CARLO SAMPLING ALGORITHM

In the present appendix, we describe the numerical algorithm used for the numerical simulations. A Monte Carlo technique has been used to sample the probability distribution of the initial wavefunctions $\phi_i^{(0)}$ and the elementary noise terms $\xi_j^{(\alpha)}(x)$.

As the effective contributions of the different realizations to the observables involve the trace of the Hartree-Fock ansatz σ , i.e. the scalar product between the two N -body Nartree-Fock states, they can have enormously different values, so a direct draw of the random variables $\phi_i^{(0)}$ and $\xi_j^{(\alpha)}(x)$ would be poorly efficient. An *importance sampling* scheme [29] has therefore been implemented, using the value of the modulus of the trace at the end $\tau = \beta$ of the imaginary-time evolution as the *a priori* probability distribution function P_0 :

$$P_0[\{\phi_i^{(0)}, \xi_j^{(\alpha)}(x)\}] = |\text{Tr}[\sigma]| = |\langle \phi_1^{(2)}(\beta) \dots \phi_N^{(2)}(\beta) | \phi_1^{(1)}(\beta) \dots \phi_N^{(1)}(\beta) \rangle|. \quad (\text{A1})$$

In this way, the contributions of the different realizations to the trace have the same absolute value, although their phases are still random.

In order to sample P_0 , a *Metropolis* scheme [30] has been implemented: at each step a random move is proposed for both the wavefunctions $\phi_i^{(0)}$ and the elementary noises $\xi_j^{(\alpha)}(x)$. For the first one, a rotation $\mathcal{R}_{\mathbf{n}\theta}$ in the one-body Hilbert space is chosen with random rotation axis \mathbf{n} and angle θ , and then is applied to all the orbitals $\phi_i^{(0)}$:

$$\phi_i'^{(0)} = \mathcal{R}_{\mathbf{n}\theta} \phi_i^{(0)} \quad (\text{A2})$$

This operation rotates the hyperplane spanned by the set of orthonormal orbitals $\{\phi_i^{(0)}\}$ describing the initial Hartree-Fock state. For what concerns the elementary noises $\xi_j^{(\alpha)}(x)$, each of them is displaced to a new position $\xi_j'^{(\alpha)}(x)$ as follows:

$$\xi_j'^{(\alpha)}(x) = \sqrt{1 - \eta^2} \xi_j^{(\alpha)}(x) + \eta b_j^{(\alpha)}(x), \quad (\text{A3})$$

$b_j^{(\alpha)}(x)$ being independent, zero-mean, complex Gaussian variables such that $\overline{b_j^{(\alpha)}(x)^2} = 0$, $\overline{|b_j^{(\alpha)}(x)|^2} = 1$. This kind of random process is such that the resulting distribution of the ξ 's is indeed a Gaussian with the required width. The parameter η as well as the probability distribution for the random rotation angle θ are free parameters which can be tuned to optimise the efficiency of the simulation. Denoting with $P_0^{(\text{in})}$ and $P_0^{(\text{fin})}$ the value of the a priori probability for the configurations respectively before and after the proposed move, this is accepted with a probability $p = \min[1, P_0^{(\text{fin})}/P_0^{(\text{in})}]$. As all configurations can be attained by the random motion and detailed balance is verified, the stationary probability distribution of the stochastic process is indeed the desired one P_0 . If a large enough number of moves is performed between successive realizations, these can be considered to be statistically independent.

APPENDIX B: EXPECTATION VALUES FOR THE CALCULATION IN THE CANONICAL ENSEMBLE

The calculation of $g_{\uparrow\downarrow}^{(2)}(x_a)$ involves the following expectation values:

$$I_n(\theta) = \langle \hat{\rho}_{\uparrow}(x_n, \tau_n) \hat{\rho}_{\downarrow}(x_n, \tau_n) \dots \hat{\rho}_{\uparrow}(x_0, \tau_0) \hat{\rho}_{\downarrow}(x_a, \tau_a) \rangle_0(\theta), \quad (\text{B1})$$

where $\hat{\rho}_{\sigma}(x, \tau) = \hat{\psi}_{\sigma}^{\dagger}(x, \tau) \hat{\psi}_{\sigma}(x, \tau)$ and $x_0 = 0, \tau_0 = \tau_a = 0$. Introducing the notations for the particle and hole correlation functions

$$P_{ij} \equiv \langle \hat{\psi}_{\uparrow}^{\dagger}(x_i, \tau_i) \hat{\psi}_{\uparrow}(x_j, \tau_j) \rangle_0(\theta) \quad (\text{B2})$$

$$H_{ij} \equiv \langle \hat{\psi}_{\uparrow}(x_i, \tau_i) \hat{\psi}_{\uparrow}^{\dagger}(x_j, \tau_j) \rangle_0(\theta) \quad (\text{B3})$$

where i, j are integers from 0 to n or are equal to a , we find

$$I_0 = P_{00}^2 \quad (\text{B4})$$

$$I_1 = (P_{00}^2 + P_{1a}H_{1a})(a \rightarrow 0) \quad (\text{B5})$$

$$I_2 = (P_{00}^3 + P_{21}H_{21}P_{00} + P_{1a}H_{1a}P_{00} + P_{2a}H_{21}H_{1a} - P_{21}H_{2a}P_{1a} + P_{2a}H_{2a}P_{00})(a \rightarrow 0) \quad (\text{B6})$$

$$I_3 = (P_{32}H_{32}P_{00}^2 + P_{32}H_{32}P_{1a}H_{1a} - P_{32}H_{31}P_{2a}H_{1a} - P_{32}H_{3a}P_{2a}P_{00} + P_{32}H_{3a}P_{21}P_{1a} - P_{32}H_{31}P_{21}P_{00} + P_{2a}H_{21}H_{1a}P_{00} + P_{2a}H_{2a}P_{00}^2 - P_{31}H_{3a}P_{1a}P_{00} + P_{3a}H_{31}H_{1a}P_{00} - P_{3a}H_{31}P_{21}H_{2a} + P_{31}H_{32}H_{21}P_{00} - P_{31}H_{32}H_{2a}P_{1a} + P_{3a}H_{3a}P_{00}^2 + P_{3a}H_{3a}P_{21}H_{21} + P_{31}H_{31}P_{2a}H_{2a} + P_{31}H_{31}P_{00}^2 + P_{00}^4 + P_{1a}H_{1a}P_{00}^2 + P_{21}H_{21}P_{00}^2 - H_{2a}P_{21}P_{1a}P_{00} + P_{3a}H_{32}H_{21}H_{1a} + P_{3a}H_{32}H_{2a}P_{00} - P_{31}H_{3a}P_{2a}H_{21})(a \rightarrow 0) \quad (\text{B7})$$

The property that each of these expressions is a product of two similar factors, the second one deduced from the first one by the replacement $a \rightarrow 0$, originates from the fact that the ideal Fermi gas in the grand canonical ensemble consists of two equivalent and independent spin components.

Similarly the calculation of $g_{\text{pair}}^{(1)}(x_a)$ involves the expectation values

$$J_n(\theta) = \langle \hat{\rho}_{\uparrow}(x_n, \tau_n) \hat{\rho}_{\downarrow}(x_n, \tau_n) \dots \hat{\psi}_{\uparrow}^{\dagger}(x_a) \hat{\psi}_{\downarrow}^{\dagger}(x_a) \hat{\psi}_{\downarrow}(0) \hat{\psi}_{\uparrow}(0) \rangle. \quad (\text{B8})$$

Using the previous notations we then obtain

$$J_0 = P_{a0}^2 \quad (\text{B9})$$

$$J_1 = (P_{00}P_{a0} + P_{10}H_{1a})^2 \quad (\text{B10})$$

$$J_2 = (P_{20}H_{21}H_{1a} + H_{2a}P_{20}P_{00} + P_{00}^2P_{a0} + P_{10}H_{1a}P_{00} + P_{a0}P_{21}H_{21} - P_{21}H_{2a}P_{10})^2 \quad (\text{B11})$$

$$J_3 = (P_{31}H_{31}P_{a0}P_{00} + P_{00}^3P_{a0} - P_{31}H_{3a}P_{10}P_{00} + P_{00}^2P_{10}H_{1a} + P_{20}H_{2a}P_{00}^2 + P_{20}H_{21}H_{1a}P_{00} - P_{21}H_{2a}P_{10}P_{00} + P_{21}H_{21}P_{00}P_{a0} + P_{30}H_{31}H_{1a}P_{00} + P_{30}H_{32}H_{2a}P_{00} + P_{32}H_{32}P_{a0}P_{00} - P_{32}H_{3a}P_{20}P_{00} + P_{31}H_{32}H_{21}P_{a0} - P_{32}H_{31}P_{21}P_{a0} + P_{32}H_{32}P_{10}H_{1a} - P_{32}H_{31}P_{20}H_{1a} + P_{32}H_{3a}P_{21}P_{10} + P_{30}H_{32}H_{21}H_{1a} - P_{30}H_{31}H_{2a}P_{21} + P_{30}H_{3a}P_{21}H_{21} - P_{31}H_{32}H_{2a}P_{10} + P_{31}H_{31}P_{20}H_{2a} - P_{31}H_{3a}H_{21}P_{20} + P_{30}H_{3a}P_{00}^2)^2. \quad (\text{B12})$$

The fact that these expressions are squares is again due to the existence of two independent and equivalent spin components.

APPENDIX C: DENSITY FLUCTUATIONS OF AN IDEAL FERMI GAS: PHYSICAL MEANING OF THE $\delta(\omega)$ TERM

The density-density correlation function for a one-component non-interacting Fermi gas in the grand canonical ensemble at inverse temperature $\beta = 1/k_B T$ and chemical potential μ can be calculated from Wick's theorem:

$$G^{(2)}(x) = \langle \hat{\rho}(x) \hat{\rho}(0) \rangle - \rho^2 = \frac{1}{L^2} \sum_{qk} e^{ikx} f_q (1 - f_{q+k}), \quad (C1)$$

where $\hat{\rho}(x)$ is the operator giving the density at point x . A calculation based on the fluctuation-dissipation theorem neglecting the term $2\pi C_{BA} \delta(\omega)$ term in (66) would give:

$$G^{(2)}(x) \stackrel{?}{=} \frac{1}{L^2} \sum_{qk}^{\neq} e^{ikx} \frac{f_q - f_{q+k}}{1 - e^{\beta(\mathcal{E}_q - \mathcal{E}_{q+k})}} \quad (C2)$$

where the sum \sum^{\neq} has to be performed over the pair of states such that $\mathcal{E}_q \neq \mathcal{E}_{q+k}$. Using the relation:

$$\frac{1 - f_q}{f_q} = e^{\beta(\mathcal{E}_q - \mu)}, \quad (C3)$$

one can see that expression (C2) does not coincide with (C1) because of the missing contribution of the pairs such that $\mathcal{E}_q = \mathcal{E}_{q+k}$.

Inclusion of the term proportional to $\delta(\omega)$ in (66) fixes the problem, since it exactly provides the missing contribution:

$$\Delta G^{(2)}(x) = \frac{1}{L^2} \sum_{qk}^{\equiv} e^{ikx} f_q (1 - f_{q+k}), \quad (C4)$$

where the sum \sum^{\equiv} has to be performed over the pairs of states such that $\mathcal{E}_q = \mathcal{E}_{q+k}$. The physical meaning of the $k = 0$ term which contains the contribution of the diagonal matrix elements of the perturbation is transparent: it keeps track of the total particle number fluctuations of the grand canonical ensemble. In our spatially homogeneous system, degenerate pairs of states for $k = -2q$ are also present.

It is apparent from (C4) that the contribution of the $\Delta G^{(2)}$ correction term tends to zero in the thermodynamical limit $L \rightarrow \infty$.

-
- [1] B. De Marco and D. S. Jin, *Science* **285**, 1703 (1999); A. C. Truscott, K. E. Strecker, W. I. McAlexander, G. B. Partridge, R. G. Hulet, *Science* **291**, 2570 (2001); F. Schreck, L. Khaykovich, K. L. Corwin, G. Ferrari, T. Bourdel, J. Cubizolles, and C. Salomon, *Phys. Rev. Lett.* **87**, 080403 (2001); S. R. Granade, M. E. Gehm, K. M. O'Hara, and J. E. Thomas, *Phys. Rev. Lett.* **88** 120405 (2002); Z. Hadzibabic, C. A. Stan, K. Dieckmann, S. Gupta, M. W. Zwierlein, A. Görlitz, and W. Ketterle, *Phys. Rev. Lett.* **88**, 160401 (2002).
- [2] J. Cubizolles, T. Bourdel, S. J. J. M. F. Kokkelmans, G. V. Shlyapnikov, and C. Salomon, *Phys. Rev. Lett.* **91**, 240401 (2003); C. A. Regal, C. Ticknor, J. L. Bohn, D. S. Jin, *Nature* **424**, 47 (2003); S. Jochim, M. Bartenstein, A. Altmeyer, G. Hendl, C. Chin, J. Hecker Denschlag, and R. Grimm, *Phys. Rev. Lett.* **91**, 240402 (2003).
- [3] M. Greiner, C. A. Regal, D. S. Jin, *Nature* **426**, 537 (2003); S. Jochim, M. Bartenstein, A. Altmeyer, G. Hendl, S. Riedl, C. Chin, J. Hecker Denschlag, and R. Grimm, *Science* **302**, 2101 (2003).
- [4] M. Bartenstein, A. Altmeyer, S. Riedl, S. Jochim, C. Chin, J. Hecker Denschlag, R. Grimm, preprint cond-mat/0401109; T. Bourdel, L. Khaykovich, J. Cubizolles, J. Zhang, F. Chevy, M. Teichmann, L. Tarruell, S.J.J.M.F. Kokkelmans, C. Salomon, preprint cond-mat/0403091.
- [5] C. A. Regal, M. Greiner, and D. S. Jin, *Phys. Rev. Lett.* **92**, 040403 (2004); M. W. Zwierlein, C. A. Stan, C. H. Schunck, S. M. F. Raupach, A. J. Kerman, and W. Ketterle, *Phys. Rev. Lett.* **92**, 120403 (2004).
- [6] P. Nozières and S. Schmitt-Rink, *J. Low. Temp. Phys.* **59**, 195 (1985)
- [7] M. Randeria, in *Bose-Einstein Condensation*, edited by A. Griffin, D. W. Snoke, and S. Stringari (Cambridge, New York, 1995), p. 355.
- [8] M. Holland, S. J. J. M. F. Kokkelmans, M. L. Chiofalo, and R. Walser, *Phys. Rev. Lett.* **87**, 120406 (2001); Y. Ohashi and A. Griffin, *Phys. Rev. Lett.* **89**, 130402 (2002); J. Carlson, S.-Y. Chang, V. R. Pandharipande, and K. E. Schmidt, *Phys. Rev. Lett.* **91**, 050401 (2003).

- [9] O. Juillet, Ph. Chomaz, D. Lacroix, and F. Gulminelli, Phys. Rev. Lett. **88**, 142503 (2002).
- [10] L. D. Landau, E. M. Lifshitz, and L. P. Pitaevskii, *Statistical Physics*, Vols.1 and 2, Pergamon Press, Oxford, 1980.
- [11] P.-G. de Gennes, *Superconductivity of metals and alloys*, Addison-Wesley, Redwood City, 1989.
- [12] A. L. Fetter and J. D. Walecka, *Quantum theory of many-particle systems*, McGraw-Hill, 1971.
- [13] G. Mahan, *Many-particle physics*, Plenum Press, New York, 1981.
- [14] J. Ruostekoski, Phys. Rev. A **60**, 1775R (1999); F. Weig and W. Zwerger, Europhys. Lett. **49**, 282 (2000).
- [15] C. Mora, Ph.D. thesis, unpublished (2004).
- [16] Y. Castin, Lecture Notes of the 2003 Les Houches School on *Quantum Gases in Low Dimensions*, EDP Sciences (2004).
- [17] see, e.g.: A. C. Aitken *Determinants and Matrices*, Oliver and Boyd, Edinburgh, 1956; F. R. Gantmacher *Theory of Matrices*, Nauka, Moscow, 1967.
- [18] O. Juillet, F. Gulminelli, Ph. Chomaz, preprint cond-mat/0311437.
- [19] for a review, see: R. R. dos Santos, Braz. J. Phys. **33**, 36 (2003) and references therein.
- [20] M. Randeria, N. Trivedi, A. Moreo, and R. T. Scalettar, Phys. Rev. Lett. **69**, 2001 (1992).
- [21] K. Kuroki, H. Aoki, Phys. Rev. B **56**, 14287 (1997); K. Kuroki, H. Aoki, J. Phys. Soc. Japan **67**, 1533 (1998).
- [22] T. Paiva, R. R. dos Santos, R. T. Scalettar, and P. J. H. Denteneer, preprint cond-mat/0403397.
- [23] R. R. dos Santos, Phys. Rev. B **50**, 635 (1994).
- [24] R. A. Ferrell, Phys. Rev. Lett. **13**, 330 (1964); S. Traven, Phys. Rev. Lett. **73**, 3451 (1994).
- [25] E. Altman, E. Demler, M. D. Lukin, preprint cond-mat/0306226
- [26] L.-P. Lévy, *Magnétisme et supraconductivité*, InterÉditions / CNRS Éditions, Paris, 1997, chapter 8.
- [27] J.-P. Blaizot and G. Ripka, *Quantum theory of finite systems*, MIT Press, 1986.
- [28] E. H. Lieb and W. Liniger, Phys. Rev. **130**, 1605 (1963).
- [29] W. H. Press, S. A. Teukolsky, W. T. Vetterling, and B. P. Flannery, *Numerical Recipes* (Cambridge University Press, Cambridge, 1988).
- [30] W. Krauth, *Introduction to Monte Carlo Algorithms*, in "Advances in Computer Simulation" (J. Kertesz and I. Kondor, eds) Lecture Notes in Physics (Springer Verlag, 1998).
- [31] In practice, a numerically more efficient formulation can be obtained from the fact that the total number of spin 1/2 fermions for a given spatial grid with \mathcal{N} points has an upper limit of $2\mathcal{N}$. If one excludes the cases $N = 0$ and $N = 2\mathcal{N}$, one can replace the integrals over θ by discrete sums over the values $\theta = 2\pi q/(2\mathcal{N})$ where the integer q ranges from 0 to $2\mathcal{N} - 1$. Furthermore, the symmetry $\sigma_{\text{gc}}(\theta)^\dagger = \sigma_{\text{gc}}(-\theta)$ may be used to reduce the range of q .
- [32] One can take e.g. $A = \|V\|(e^{\beta\Delta E_0} - 1)/\Delta E_0$ where ΔE_0 is the difference between the largest and the smallest eigenvalues of $\mathcal{H}_0 - \mu_0\hat{N}$ and where the norm of V is $\|V\| \leq |g_0|L/dx^2$.
- [33] Each term of the perturbative expansion is expected to diverge in the $T \rightarrow 0$ limit; this can be checked to be the case for the first order correction to $g_{\uparrow\downarrow}^{(2)}(0)$ in the grand canonical ensemble, this correction diverging as $-\beta g_0/L$. We therefore restrict the perturbative expansion to temperatures larger than $|g_0|/L \sim 10$ in dimensionless units.
- [34] A simpler expression for the denominator of the second order term is $\partial_{\mu_0}\rho_{0\uparrow}$ where $\rho_{0\uparrow}$ is the density in one spin component of the ideal Fermi gas with a chemical potential μ_0 .
- [35] A remark useful for the calculations to come is to realize that $\tilde{\chi}_{BA}(\omega)$ has no delta singularity in $\omega = 0$.
- [36] Our expression of Ω in terms of a Matsubara sum differs from the unnumbered equation between Eqs. (19) and (20) of [6]. This is due to the omission by the authors of [6] of the contribution to the contour integral of the half-circle of infinite radius in the $\text{Re}\omega < 0$ half plane.
- [37] The situation is more subtle in 3D: in the model of [7], the bare coupling constant g_0 tends to zero when the cut-off energy tends to infinity, in which case the Hartree-Fock mean field term in μ_{NSR} tends to zero. In this regime, a non-perturbative resummation procedure then seems unavoidable.